Available online at www.sciencedirect.com
ScienceDirect
Icarus 190 (2007) 74–92
ICARUS
www.elsevier.com/locate/icarus

Possible ancient giant basin and related water enrichment in the Arabia Terra province, Mars

James M. Dohm [a,b,*], Nadine G. Barlow [c], Robert C. Anderson [d], Jean-Pierre Williams [e], Hirdy Miyamoto [f,g], Justin C. Ferris [h], Robert G. Strom [b], G. Jeffrey Taylor [i], Alberto G. Fairén [j,k], Victor R. Baker [a,b], William V. Boynton [b], John M. Keller [b], Kris Kerry [b], Daniel Janes [b], J.A.P. Rodriguez [l], Trent M. Hare [m]

[a] *Department of Hydrology and Water Resources, University of Arizona, Tucson, AZ 85721, USA*
[b] *Lunar and Planetary Laboratory, University of Arizona, Tucson, AZ 85721, USA*
[c] *Department of Physics and Astronomy, Northern Arizona University, Flagstaff, AZ 86011, USA*
[d] *Jet Propulsion Laboratory, California Institute of Technology, Pasadena, CA 91109, USA*
[e] *Division of Geological and Planetary Sciences, California Institute of Technology, Pasadena, CA 91125, USA*
[f] *The University Museum, University of Tokyo, Tokyo 113-0033, Japan*
[g] *Department of Earth and Planetary Science, University of Tokyo, 7-3-1 Hongo, Bunkyo-ku, Tokyo 113-0033, Japan*
[h] *National Weather Service, National Oceanic and Atmospheric Administration, Palmer, AK 99645, USA*
[i] *Hawai'i Institute of Geophysics and Planetology, University of Hawai'i, Honolulu, HI 96822, USA*
[j] *Centro de Biología Molecular, CSIC-Universidad Autónoma de Madrid, 28049 Cantoblanoc, Madrid, Spain*
[k] *Space Science and Astrobiology Division, NASA Ames Research Center, Moffett Field, CA 94035, USA*
[l] *Planetary Science Institute, 1700 East Ft. Lowell Rd., Suite 106, Tucson, AZ 85719, USA*
[m] *United States Geological Survey, Flagstaff, AZ 86001, USA*

Received 24 August 2006; revised 26 February 2007

Available online 28 March 2007

Abstract

A circular albedo feature in the Arabia Terra province was first hypothesized as an ancient impact basin using Viking-era information. To test this unpublished hypothesis, we have analyzed the Viking era-information together with layers of new data derived from the Mars Global Surveyor (MGS) and Mars Odyssey (MO) missions. Our analysis indicates that Arabia Terra is an ancient geologic province of Mars with many distinct characteristics, including predominantly Noachian materials, a unique part of the highland–lowland boundary, a prominent paleotectonic history, the largest region of fretted terrain on the planet, outflow channels with no obvious origins, extensive exposures of eroded layered sedimentary deposits, and notable structural, albedo, thermal inertia, gravity, magnetic, and elemental signatures. The province also is marked by special impact crater morphologies, which suggest a persistent volatile-rich substrate. No one characteristic provides definitive answers to the dominant event(s) that shaped this unique province. Collectively the characteristics reported here support the following hypothesized sequence of events in Arabia Terra: (1) an enormous basin, possibly of impact origin, formed early in martian history when the magnetic dynamo was active and the lithosphere was relatively thin, (2) sediments and other materials were deposited in the basin during high erosion rates while maintaining isostatic equilibrium, (3) sediments became water enriched during the Noachian Period, and (4) basin materials were uplifted in response to the growth of the Tharsis Bulge, resulting in differential erosion exposing ancient stratigraphic sequences. Parts of the ancient basin remain water-enriched to the present day.

Keywords: Mars; Geological processes; Geophysics; Impact processes; Tectonics

1. Introduction

Distinct geologic provinces at regional scales on Mars provide windows into the recorded history of the planet. This

* Corresponding author.
E-mail address: jmd@hwr.arizona.edu (J.M. Dohm).

0019-1035/$ – see front matter
doi:10.1016/j.icarus.2007.03.006

includes the ancient geologic provinces that typically display highly degraded macrostructures (tectonic features tens to thousands of kilometers long) and degraded promontories among distinct magnetic signatures (e.g., Dohm et al., 2002, 2005; Connerney et al., 2005). Here, "early" or "ancient" refers to the oldest part of the recorded history of Mars exposed at or near its surface, representing the late heavy bombardment period (roughly older than 3.8 Ga). These ancient provinces may record an extremely active planet during its early development, possibly including plate tectonics driven by internal activity which also produced an active magnetic dynamo and magnetosphere (Baker et al., 2002; Fairén and Dohm, 2004; Connerney et al., 2005) pre-dating the Hellas and Argyre impact events (Acuña et al., 1999, 2001; Arkani-Hamed, 2003; Connerney et al., 1999, 2005). One particularly unique window into the ancient past is located northwest of the Hellas impact basin in the Arabia Terra province, occurring between the equator and 40° N latitude and within the 0°–60° E longitude zone. A circular albedo feature in the Arabia Terra province, which is partly surrounded by the younger Hellas impact basin to the southeast, the Isidis impact basin and volcanics of Syrtis Major to the east, and the dichotomy boundary to the north-northwest, is hypothesized to mark an ancient basin (Fig. 1), forming the basis of this investigation. In order to test this Viking-based, unpublished hypothesis, we have compiled and analyzed layers of information derived from the Mars Global Surveyor (MGS) and Mars Odyssey (MO) missions to see whether the new information supports the basin hypothesis.

The Arabia Terra province is one of the few visible water-rich equatorial regions of Mars, as indicated by impact crater (Barlow and Perez, 2003) and elemental (Boynton et al., 2002; Feldman et al., 2002a) analyses. This region records many unique characteristics, including:

- The largest portion of heavily cratered terrain in the martian northern hemisphere.
- Mostly Noachian materials, as indicated by its high crater density (Tanaka, 1986; Greeley and Guest, 1987; Barlow, 1988).
- A highland–lowland dichotomy boundary region that is distinct from other boundary regions by displaying extensive denudation (Hynek and Phillips, 2001).
- Some of the lowest topography displayed in the heavily cratered region of the planet (Smith et al., 2001).
- A distinct center of tectonic activity based on wrinkle ridge information of the eastern equatorial region (Anderson et al., 2006).

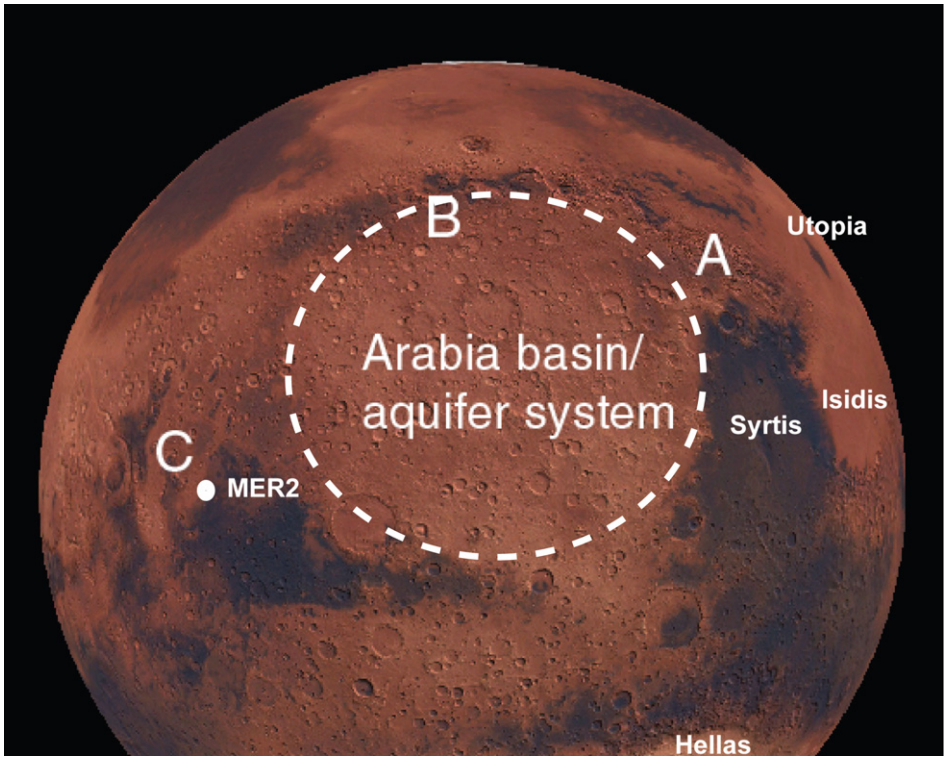

Fig. 1. Circular light-albedo feature approximates the primary basin of the proposed ancient Arabia Terra basin, possibly impact in origin, which is at least 1.5 times the size of Hellas (the primary basin is approximated by dots in Figs. 3, 10, 12–13). If an ancient basin, the lighter albedo materials could represent light albedo sedimentary deposits (including evaporite deposits) compared to the darker volcanic materials of the Syrtis volcanic province to the east. Another possibility is ice deposition, which is possible in the Arabia Terra province since it is a region characterized by low thermal inertia (Christensen et al., 2001) (for more detail, see Section 2.6). Also shown are: (1) the largest region of fretted terrain on Mars (A: also see corresponding Fig. 6), (2) outflow channels such as Mamers Valles that initiate near the possible rim region of the ancient impact structure (a previously indistinct source region) and debouch in the Deuteronilus Mensae region of the northern plains (B: also see corresponding Fig. 7), and (3) distinct anastomosing-patterned albedo features that are interpreted to mark ancient paleodrainages that debouch into the impact basin region (C: also see corresponding Fig. 8); "C" also marks approximate location of Fig. 2. Also shown are the locations of the MER-2 (Opportunity rover) landing site, Hellas, Isidis, and Utopia basins, and the Syrtis volcanic province.

- Very few macrostructures when compared to the rest of the cratered highlands (Dohm et al., 2002).
- The greatest extent of well-developed fretted terrain on Mars (Sharp, 1973; Scott et al., 1995; Carr, 2001).
- Outflow channels, such as Mamers Valles, that have no obvious source regions (Scott et al., 1995).
- A high concentration of multiple layer ejecta and central pit impact craters, suggesting a concentration of volatile-rich materials (Barlow and Perez, 2003).
- Higher albedo than the surrounding highland provinces of Syrtis Major, Terra Sabaea, Terra Meridiani, and Terra Margaritifer (US Geological Survey, 1991).
- Lower thermal inertia than its surroundings (Christensen et al., 2001).
- A free-air gravity signal that is uniform relative to the rest of the cratered highlands (Yuan et al., 2001).
- Presence of distinct magnetic anomalies (Acuña et al., 1999, 2001; Connerney et al., 1999, 2005; Arkani-Hamed, 2003).
- Unique elemental signatures for H_2O and Cl (Boynton et al., 2002, 2004, 2007; Feldman et al., 2002a).

The large array of unique characteristics supports Arabia Terra as being the site of an ancient giant basin, possibly of exogenic (impact) or endogenic (paleotectonic) origin, that later became an important and long-lived site of water enrichment, perhaps in the form of regional and/or perched aquifers. The characteristics and implications of the proposed basin, centered near 15° N 30° E and estimated to be at least 3000 km in diameter (∼1.5 times the size of Hellas), are detailed below.

2. Special characteristics of Arabia Terra

Based on the Viking-era hypothesis of an ancient impact basin within the Arabia Terra region, we have compiled layers of information derived from the Mars Global Surveyor (MGS) and Mars Odyssey (MO) missions to see whether the new information are consistent with the basin hypothesis. It is beyond the scope of this work, however, to explain and present multiple hypotheses for each characteristic.

2.1. Stratigraphy

The proposed Arabia Terra basin consists of more than 95% Noachian terrain, which indicates an ancient time of emplacement for the rock materials of the province. The materials have been mapped and described using Viking data at 1:15,000,000 scale as the hilly (Nplh), ridged (Nplr), etched (Nple), dissected (Npld), cratered (Npl_1), and subdued cratered (Npl_2) units of the Plateau Sequence (Greeley and Guest, 1987). More recent mapping at the 1:1,000,000 scale describes these materials as knobby and ridged (Nkr), highland terrain (Nht), knob (Nk), dark plateau (Npld), hummocky plateau (Nplh), smooth plateau (Npls), butte (NHb), and rough lowland (NHrl) materials of the basement and plateau materials (McGill, 2002). These highland materials have been interpreted to consist of impact breccia, volcanic materials, and sedimentary deposits of possible eolian, fluvial, marine, glacial, and colluvial origin (e.g., Tanaka, 1986; Greeley and Guest, 1987; McGill, 2002; Fairén et al., 2003).

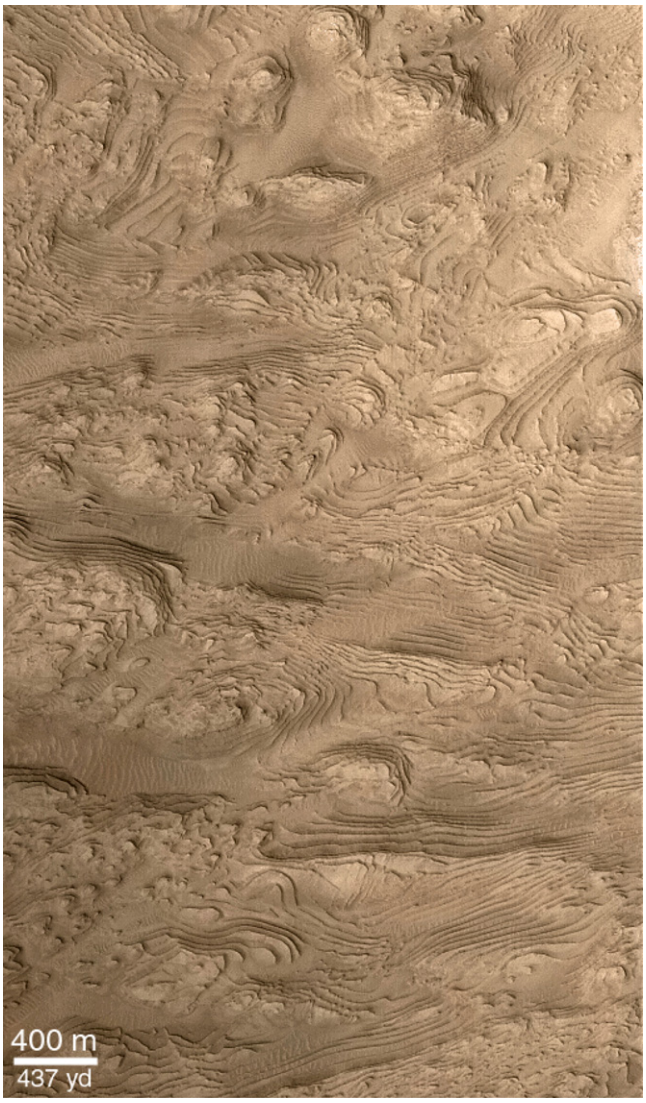

Fig. 2. "Colorized" subframe MOC M14-01647 (from Malin Space Science Systems) showing exhumed sedimentary deposits in a 64 km-wide impact crater located in western Arabia Terra at 8° N, 7° W (Malin and Edgett, 2000); the layered deposits may mark the ancient Arabia Terra basin system, especially if the proposed Arabia Terra impact basin was a multi-ringed structure.

Water appears to have played a major role in the evolution of Arabia Terra. MGS's Mars Orbiter Camera (MOC) imagery, for example, clearly reveals layered deposits in the Arabia Terra and nearby Meridiani Planum regions (Malin and Edgett, 2000, 2001, 2003; Edgett and Malin, 2002; Edgett, 2005) (Fig. 2). On Earth, such sequences typically form in basins. Two sequences of extensive layered materials have been recognized (Tanaka et al., 2004): (1) relatively indurated layers exposed in crater and channel walls, which date from the early to middle Noachian period, and (2) Late Noachian and younger friable layers superposed on degraded craters and commonly eroded into yardangs. The continuity of these layered geologic units is consistent with the upper crustal materials of Arabia Terra and Meridiani Planum being deposited in one or more ancient topo-

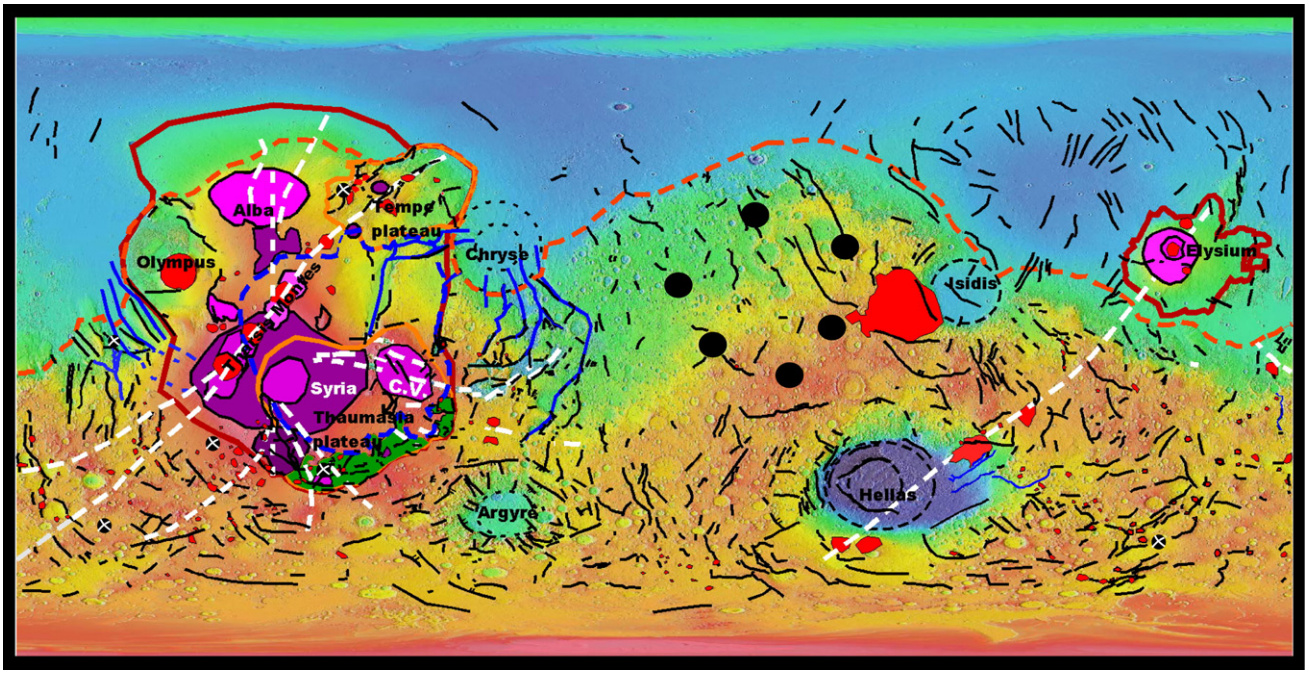

Fig. 3. Map showing proposed primary ancient basin (dotted circle) with respect to macrostructures (topography courtesy of MOLA team; high regions in red and yellow hues while low in shades of blue); revised from Dohm et al. (2002). Note that there are fewer macrostructures in the proposed basin system region, interpreted here to reflect basement structural control and sediment fill of an ancient impact basin. Most macrostructures are interpreted to be the result of pre-Tharsis superplume plate tectonism, giant impacts (e.g., Chryse, Argyre, Hellas, Isidis), and Tharsis superplume activity. Also shown are Tharsis and Elysium superplumes (red lines), highland–lowland boundary (orange dashes), structural weakness in crust/lithosphere (white dashes), extensional, thrust, and/or transform faults (black lines), Tempe and Thaumasia igneous plateaus (orange lines), Thaumasia highlands and Coprates rise mountain ranges (green patterns), magmatic-driven structural landform complexes of Tharsis superplume (irregular shapes colored in varying shades of violet—see Dohm et al., 2001b, for relative age of formation), promontories, which are interpreted to be shield volcanoes, silicic-rich lava domes (e.g., andesitic domes), highly-degraded intrusives, and impact-related massifs (red quasi-circular patterns), outflow channels (blue lines), and Tharsis superplume basin system (Dohm et al., 2001b) (dashed blue line).

graphic lows (paleobasins). The ancient sedimentary sequences of Arabia Terra and Meridiani Planum record relatively high erosion rates that competed with high rates of crater formation during the late heavy bombardment period (Baker et al., 2002). These deposits have been exposed by uplift and differential erosion, perhaps associated with the growth of the Tharsis bulge (Phillips et al., 2001). If impact influenced, Arabia Terra is interpreted here to be the site of the primary basin (Figs. 1 and 3) and Meridiani Planum a part of a greater deformational extent of the putative giant impact (e.g., part of a multi-ringed structure). If paleotectonic influenced (Connerney et al., 2005), both regions could be part of a complex of basins associated with spreading centers.

2.2. Topography

The proposed ancient Arabia Terra basin is not directly apparent using Mars Orbiter Laser Altimeter (MOLA) topography data (Fig. 3). However, this is not unexpected due to the extreme age of the putative basin. There are topographic subtleties, which suggest the basin's presence. These include: (1) the lowest part of the ancient heavily cratered terrain on Mars with elevations ranging between −3 km to +1 km compared to the +1 to +4 range of the rest of the cratered uplands (only the floors of large impact basins such as Hellas and Argyre are lower), and (2) a unique dichotomy boundary region when compared to other boundary regions, as the western and northern parts of the proposed primary basin display a more gradual topographic transition between the cratered highlands and lowlands (Figs. 3 and 4). The broad gentle slope may be indicative of erosion of laterally consistent geologic materials, consistent with sedimentary basin fill. In addition, Arabia Terra is also unique from a MOLA-based, crustal thickness perspective (see Zuber et al., 2000). As ancient topography (e.g., Early and Middle Noachian epochs) may have been strikingly different from present-day topography due to several factors such as thermal isostasy and erosion (Fairén et al., 2003; Ruiz et al., 2004), a basin, possibly impact induced, could explain why the Arabia Terra region is reported to be underpinned by relatively thin crust when compared to other parts of the cratered highlands.

2.3. Paleotectonics

The tectonic history of a planet is recorded in the distribution and relative age of extensional and contractional features (graben and wrinkle ridges, respectively) that can be mapped on its surface. In order to assess the tectonic history of Mars, the work of Anderson et al. (2001) for the western hemisphere has been extended to include the eastern hemisphere (Anderson et al., 2006). Many studies have established the overall histories of specific geologic provinces for the eastern hemisphere, which includes the Elysium rise (e.g., Greeley and Guest, 1987; Tanaka et al., 2003, 2005), but no study has systemat-

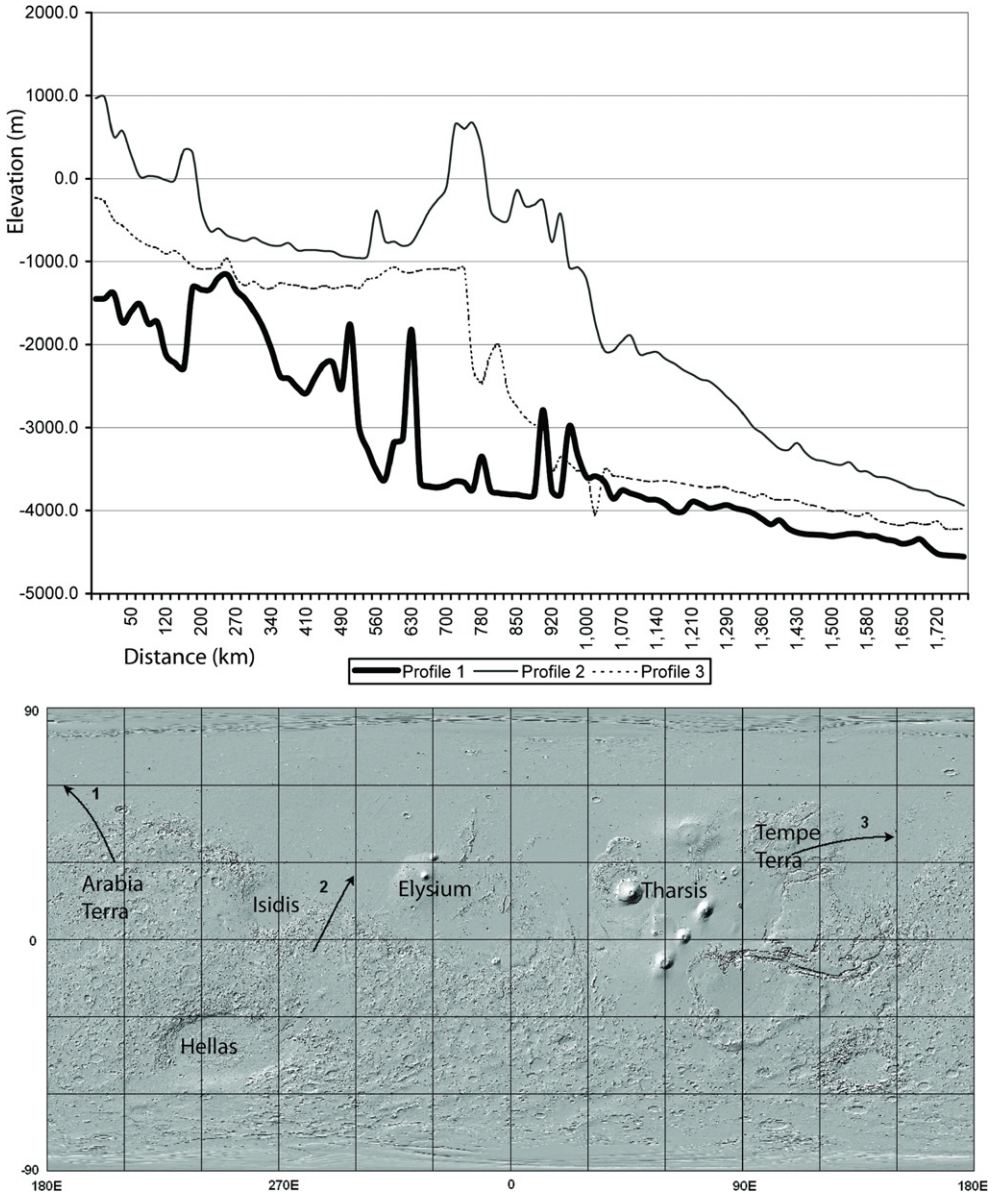

Fig. 4. MOLA shaded relief map (below) with topographic profile transects shown (arrows indicate decreasing elevations), corresponding to Profiles 1–3 (above). The three profiles transect the highland–lowland boundary at three different locations for general comparative analysis among the northwest part of Arabia Terra, Isidis-east, and Tempe Terra. Note that the Profile 1 (transecting Arabia Terra) is distinct from Profiles 2–3 (Isidis-east and Tempe Terra, respectively), particularly as it displays a more gradational transition between the cratered highlands and lowlands.

ically placed the tectonic structures into a hemispheric stratigraphic framework. In the Anderson et al. (2006) investigation of the eastern hemisphere, over 22,000 tectonic features were mapped, classified, digitized, and analyzed using the Vector Analysis approach (similar to the approach used in Anderson et al., 2001).

Based on the comprehensive paleotectonic investigation of the eastern hemisphere (Anderson et al., 2006), dominant centers of tectonic activity correspond with the Elysium rise and Hadriaca/Tyrrhena volcanic provinces (including Hellas), Isidis (including Syrtis Major), and Arabia Terra regions. While a radiating system of graben sources from the Elysium rise, normals from thousands of wrinkle ridges point back to centers of tectonism within the Hadriaca/Tyrrhena volcanic provinces, Isidis, and Arabia Terra regions (Anderson et al., 2006) (Fig. 5) based on the interpretation that all wrinkle ridges represent thrust faults (e.g., Plescia and Golombek, 1986; Watters and Maxwell, 1986; Watters, 1988; Golombek et al., 1991). Though the Arabia Terra center of tectonism is not a confirmation of a giant ancient impact, the center is consistent with such a proposed event; an impact event would produce a complex structural fabric in the lithosphere/crust, comprising structural features that could be subsequently reactivated by other stresses. Contributions to the observed center of tectonic activity may include regional uplift related to the growth of Tharsis (Phillips et al., 2001), planetary cooling-related contraction (e.g., Barosio et al., 2002), and plate tectonism (Connerney et al., 2005), all of which may not be mutually exclusive.

In addition to the Arabia Terra center of tectonic activity revealed through the Anderson et al. investigation, detailed

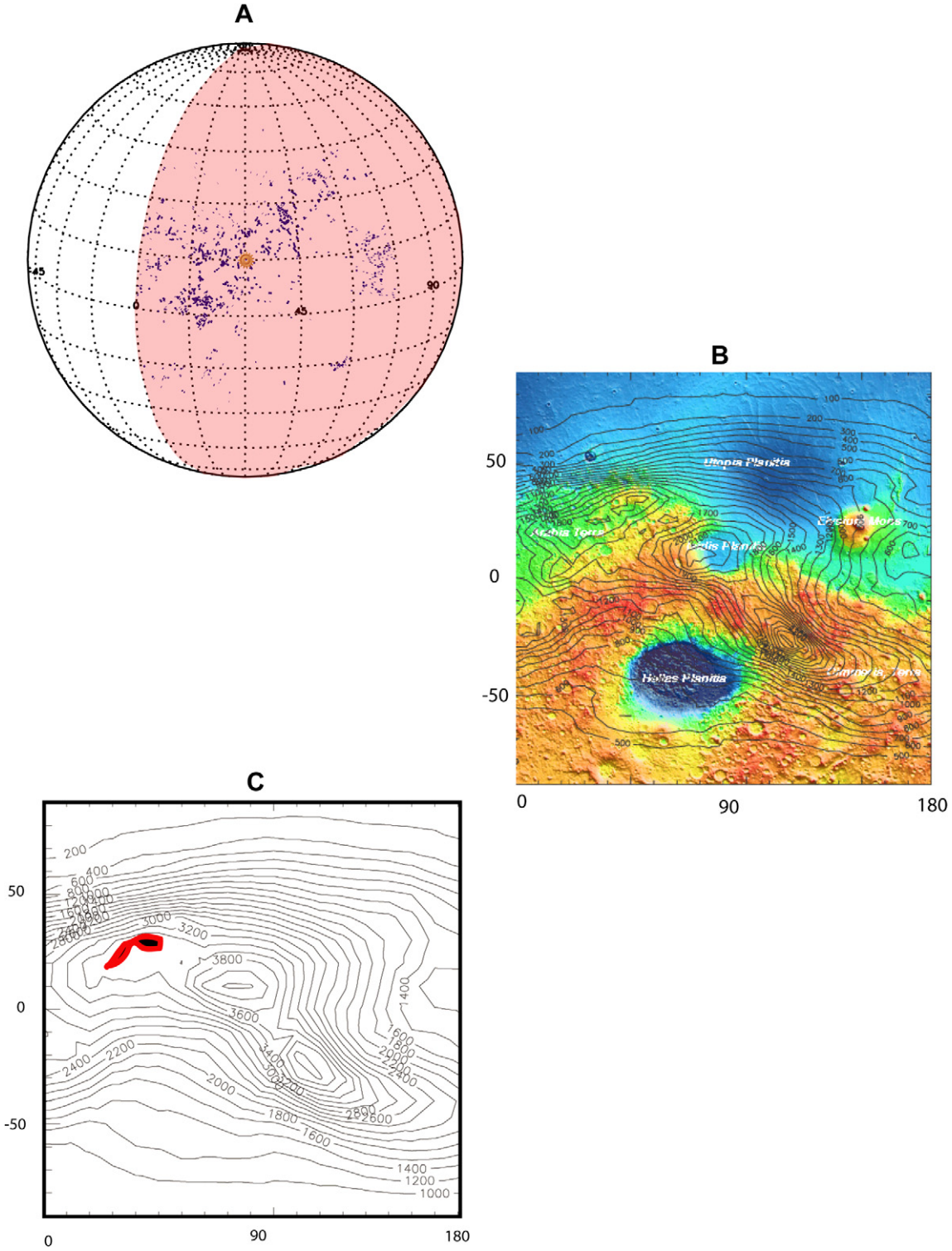

Fig. 5. (A) Wrinkle ridges with normals that trace back to the Arabia Terra center of tectonism (Gold Star) of the eastern hemisphere of Mars (Anderson et al., 2006); pink shaded area represents surface area covered in Figs. 5B and 5C. (B) Contour plot on MOLA topography showing the three primary centers of compressional tectonic activity for the eastern hemisphere (Anderson et al., 2006) (contour interval represents density of intersections of 200 wrinkle ridge intersections; center is identified by the normals of 2701 wrinkle ridges, which trace back to Arabia Terra, or 18% of the total ridges identified for the eastern hemisphere of Mars). (C) Similar to (B), but without the MOLA background (red highlighted area shows the approximated Arabia Terra center).

structural mapping using high-resolution MOLA topographic data reveals fewer macrostructures within the proposed Arabia Terra basin region when compared to other ancient parts of the cratered highlands (Fig. 3). The term macrostructure refers to an extremely large (tens to thousands of kilometers in length) tectonically-induced dislocation in the martian crust (Dohm et al., 2002, 2004). Observed features within the Arabia Terra province include a few macrostructures from Hellas, a small

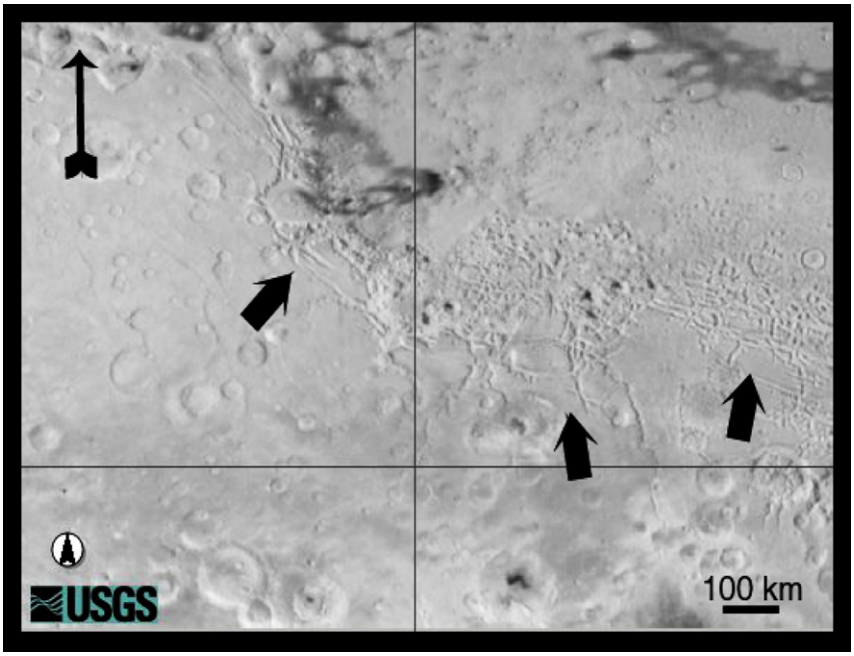

Fig. 6. Mars Digital Image Mosaic (bottom right—71.7° E, 25.6° N; top left—49.1° E, 41.4° N) showing the most extensive occurrence of fretted terrain on Mars located on the northeast margin of the hypothesized ancient Arabia Terra basin (arrows; also see "A" of Figs. 1 and 8 for regional context). This is the largest extent of fretted terrain on Mars, and is interpreted to have formed in part due to the complex structural fabric in the crust/lithosphere resulting from the overlap of Utopia, Isidis, and the proposed Arabia Terra impact basins, which would increase the hydraulic conductivity of the region (e.g., Rodriguez et al., 2005b).

number possibly associated with the development of the Utopia and Isidis impact basins, and some that may be related to an extremely ancient phase of plate tectonics (Baker et al., 2002; Dohm et al., 2002; Fairén et al., 2002; Fairén and Dohm, 2004). Even though Utopia Planitia has been reported as an ancient impact structure that has been obscured largely by burial (McGill, 1989), impact-related macrostructures are more numerous than Hellas-related macrostructures in the region extending to the north-northwest of the large basin into the Arabia Terra province.

Why is there a paucity of Hellas-induced tectonic structures in this particular region? To explain this simply by resurfacing (both degradation and aggradation) is tenuous, since the macrostructures are observed to be more prevalent along the southern and eastern margins of the Hellas impact basin where major water, wind, and volcanic activity are reported (Greeley and Guest, 1987; Kargel and Strom, 1992; Crown et al., 1992; Scott et al., 1995; Moore and Wilhelms, 2001; Head and Pratt, 2001; Tanaka et al., 2002). On the other hand, if the proposed basin originated from impact, then this apparent paucity could be more easily explained by an impact-induced complex basement structural fabric of the crust and lithosphere (e.g., pre-basin floor materials). This structurally complex basement would subsequently become buried by thick basin infill. The immense energy of a subsequent Hellas impact would be transferred along the complex fabric (dissipating affect), limiting the total number of Hellas-induced structures.

2.4. Geomorphology/paleohydrology

Rock materials of the Arabia Terra province and surrounding regions have been highly denudated (Hynek and Phillips, 2001), consistent with the broad gradational transition in MOLA-based topography between the cratered highlands and lowlands when compared to other parts of the highland–lowland dichotomy (Figs. 3 and 4). Denudation has exposed ancient stratigraphic sequences and older features such as previously buried impact craters and old paleodrainages (Malin and Edgett, 2000, 2001, 2003; Edgett and Malin, 2002). These features may have been exposed in response to uplift related to the growth of antipodal Tharsis (Phillips et al., 2001) and associated differential erosion from wind and water.

This region includes the largest concentration of fretted terrain on Mars, located on the northeastern margin of the Arabia Terra province (Figs. 1 and 6) (Sharp, 1973; Sharp and Malin, 1975; McGill, 2002). The fretted terrain lies at the intersecting margins of the proposed Arabia Terra basin and the Isidis and Utopia impact basins. Hydraulic conductivity is expected to be elevated at the margins of adjoining basins/craters due to fracturing within the rims, resulting in enhanced degradation of overlapping rim materials (Rodriguez et al., 2005a, 2005b). These processes are analogous to those demonstrated on Earth, where basement structures act as conduits for the flow of surface and subsurface water (e.g., Dohm et al., 2001a). The enhanced water flow in the region would further erode the rim materials, which includes both surface (e.g., Scott et al., 1995; Hynek and Phillips, 2001) and subsurface flow to the north in response to gravitational gradients and the migration of volatiles along impact-induced fractures and faults, contributing to the formation of the fretted terrain.

The indistinct source region of Hesperian-aged Mamers Valles and other nearby outflow channels that debouch into Deuteronilus Mensae (Scott et al., 1995) (Figs. 1 and 7) can be

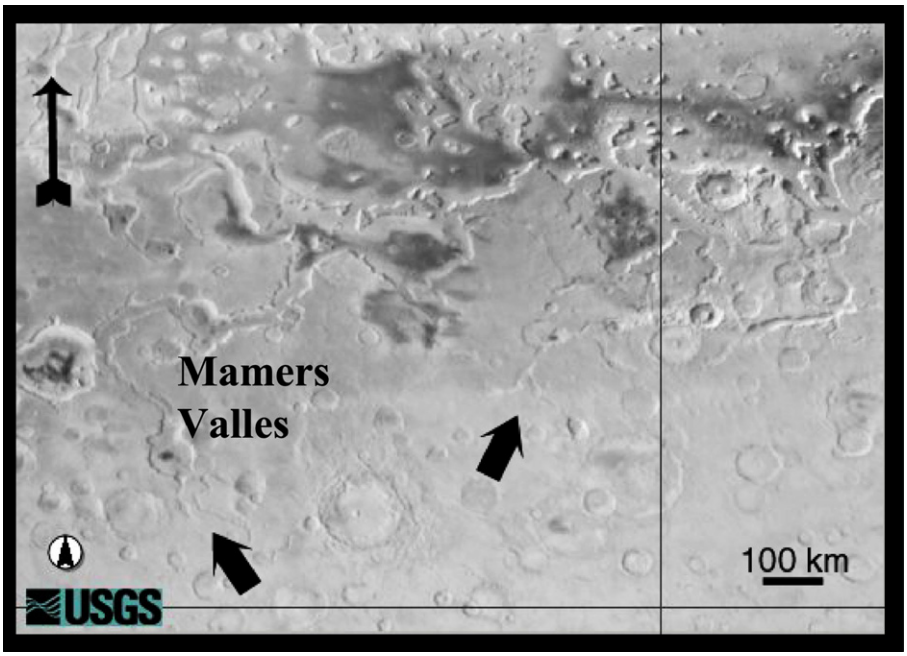

Fig. 7. Mars Digital Image Mosaic (bottom right—35.8° E, 28.9° N; top left—13.2° E, 45.6° N) showing the indistinct source region of Mamers Valles (arrows mark approximate source regions, which occur in the crater rim region of the proposed Arabia Terra impact basin) and other nearby outflow channels, as observed through Viking imagery. These outflow channel systems that debouch into the Deuteronilus Mensae region may be explained by their location with respect to the northern margin of a productive ancient impact basin/aquifer system (also see "B" of Fig. 1 for location).

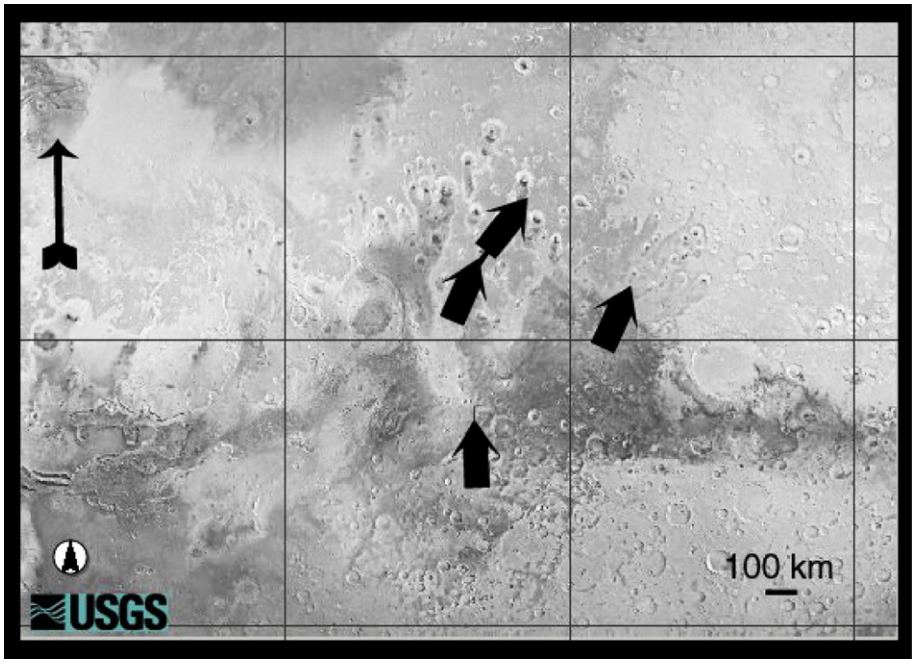

Fig. 8. Mars Digital Image Mosaic (bottom right—34.0° E, 31.5° S; top left—301.5° E, 33.3° N) showing albedo features (arrows) interpreted here to mark ancient paleodrainages that debouched into the Arabia Terra basin region, highlighting a productive Noachian basin system (see "C" of Fig. 1 for location).

explained by their location with respect to the northern margin of water-rich sediments associated with a basin in the Arabia Terra province. Distinct albedo features on the southwestern margin of the proposed basin near the Opportunity landing site (Figs. 1 and 8) appear to be ancient paleodrainages that debouch into the Arabia Terra basin. The diverse paleohydrologic history of the Arabia Terra region also is consistent with post-basin water inundation from a putative Noachian ocean, which is estimated to have covered 1/3 of the total surface area of the planet (Fairén et al., 2003), as well as a multitude of water-related features observed at the Opportunity landing site (Fairén et al., 2004; Squyres et al., 2004).

Table 1
Percentage of SLE, DLE, and MLE craters relative to all craters showing any type of ejecta morphology within 10° latitude by 10° longitude blocks surrounding Arabia Terra

	350–360E	0–10E	10–20E	20–30E	30–40E	40–50E	50–60E
				SLE craters			
40N–50N	14	21	50	44	50	33	42
30N–40N	73	70	88	72	75	80	86
20N–30N	75	92	77	76	100	69	80
10N–20N	69	80	69	84	78	86	83
0–10N	74	84	100	87	80	95	91
10S–0	71	90	88	89	93	93	82
20S–10S	100	96	95	88	73	100	97
				DLE craters			
40N–50N	81	79	44	33	50	58	50
30N–40N	16	7	10	9	0	0	0
20N–30N	4	0	0	0	0	0	0
10N–20N	0	0	3	0	0	0	0
0–10N	0	0	0	0	0	0	0
10S–0	0	0	4	0	0	0	0
20S–10S	0	0	0	0	0	0	0
				MLE craters			
40N–50N	5	0	6	22	0	0	8
30N–40N	10	20	2	16	25	26	10
20N–30N	20	4	19	18	0	8	13
10N–20N	24	13	21	14	17	14	8
0–10N	21	12	0	3	20	5	4
10S–0	7	5	0	5	3	4	8
20S–10S	0	0	5	8	5	0	0

The shaded boxes correspond to the areas covered by the Arabia Terra basin. Each box contains an average of 35 craters displaying some type of ejecta morphology.

2.5. Impact crater record

Impact craters within the Arabia Terra province display a number of unusual characteristics. These features include ejecta and interior structures, which suggest crater formation in volatile-rich target materials. The range of preservation states of these crater features indicates that the volatile-rich materials have persisted over a substantial period of martian history up to the present time.

2.5.1. Crater morphology

Fresh impact craters on Mars are surrounded by a variety of ejecta blanket morphologies, most of which display characteristics of emplacement by flow processes (Mouginis-Mark, 1979; Costard, 1989; Barlow and Bradley, 1990). Ejecta displaying these fluidized appearances are called "layered ejecta morphologies" and are further characterized by the number of identifiable ejecta deposits as "single layer ejecta" (SLE; one ejecta layer), "double layer ejecta" (DLE; two complete ejecta layers), or "multiple layer ejecta" (MLE; three or more partial or complete ejecta layers) (Barlow et al., 2000). A global analysis using Viking and MOC data revealed that SLE craters dominate in most regions of the planet (constituting 83% of all craters displaying an ejecta pattern) with DLE and MLE craters showing regional concentrations (Barlow and Perez, 2003). Globally, 9% of all ejecta craters display a DLE morphology and 5% are MLE. The northern portion of Arabia Terra was one of the regions reported as displaying an enhanced concentration of MLE morphology craters (Barlow and Perez, 2003).

A renewed examination of impact craters in Arabia Terra using MO's Thermal Emission Imaging System (THEMIS) visible (VIS) and daytime infrared (IR) imagery reveals a large number of craters displaying a layered ejecta morphology because of higher resolutions (Barlow, 2005a). Some craters which were classified with SLE morphology based on Viking analysis are shown to actually be MLE craters in THEMIS data. In addition, many craters which were not classified with an ejecta morphology or whose ejecta morphology was ambiguous in Viking data are able to be classified using THEMIS analysis. Ejecta morphologies of approximately 25% of the craters examined to date have been revised based on THEMIS analysis.

Globally within the 0° to 40° N zone we find that SLE craters constitute 84% of all the ejecta craters $\geqslant$5-km-diameter and DLE and MLE craters makes up 5 and 7%, respectively. Within Arabia Terra the numbers are 83% SLE, 5% DLE, and 12% MLE, indicating a slight enhancement of MLE morphologies compared to the global average (Table 1). SLE craters are found throughout the proposed Arabia Terra basin and do not show any statistically significant variation from the concentration of SLE craters in surrounding regions. DLE craters are concentrated outside of the Arabia Terra basin region, particularly in the plains north of the basin. MLE craters are concentrated within the northern part of the basin and to the west. Within the basin, SLE craters dominate over MLE or DLE.

Two models have been proposed to explain the layered ejecta morphologies on Mars: impact into and vaporization of subsurface volatiles (Carr et al., 1977; Wohletz and Sheridan, 1983; Stewart et al., 2001), and ejecta curtain interaction with the martian atmosphere (Schultz and Gault, 1979; Schultz, 1992; Barnouin-Jha et al., 1999a, 1999b). A substantial amount of observational, laboratory, and numerical evidence supports the theory that subsurface volatiles play a dominant role in the

formation of the layered ejecta morphologies (see review in Barlow, 2005b); this is the mechanism we invoke in the interpretation of crater morphology data in Arabia Terra.

SLE craters are generally believed to form by impact into ice-rich targets while DLE craters may be produced by excavation into layered target materials such as sedimentary deposits (Mouginis-Mark, 1979, 1987; Costard, 1989; Barlow and Bradley, 1990; Barlow and Perez, 2003; Stewart et al., 2001). The MLE morphology has been proposed to result either from excavation into liquid reservoirs (Wohletz and Sheridan, 1983; Barlow and Bradley, 1990) or by interaction of a volatile-rich ejecta curtain with the martian atmosphere (S. Stewart, personal communication). The regional concentrations of MLE morphology craters (Mouginis-Mark, 1979; Barlow and Bradley, 1990; Barlow and Perez, 2003), their association with other features purported to be indicators of a volatile-rich substrate (Barlow and Perez, 2003), and their correlation with the high-water abundance equatorial regions revealed by Odyssey's Gamma Ray Spectrometer/Neutron Spectrometer (GRS/NS) data (Boynton et al., 2002; Barlow and Perez, 2003) provide strong circumstantial support that subsurface volatiles are likely involved in their formation and that conditions are different in these regions than where SLE craters dominate.

SLE craters within the Arabia Terra region range in size from 3 km to almost 50 km in diameter, with an average diameter of 10.4 km. DLE craters are found in the 4 to 26 km diameter range with an average size of 10.7. The MLE morphology is typically associated with larger craters, ranging in size from 8 to 59 km, with an average diameter of 27 km. Depth–diameter relationships allow us to estimate the depths of excavation of these craters and thus constrain the depths to the potential volatile reservoirs. MOLA-based analyses of impact crater morphometries, together with empirical relationships between transient and observed crater rim diameters, gives the following relationship between excavated depth (d_e) and apparent crater diameter (D_a) for fresh impact craters on Mars (Garvin et al., 2000):

$$d_e = 0.131 D_a^{0.85}. \quad (1)$$

Using this relationship, we find that SLE and DLE craters within the Arabia Terra province are excavating to an average depth of about 1 km while MLE craters are excavating to about 2 km depth. While the ejecta deposits are primarily derived from the top 1/3 of the crater excavation depth, volatiles at greater depths could be vaporized during crater formation and interact with the ejecta (Barlow et al., 2001). Thus, we take the above calculated depths as average depths of the ice and possible liquid water reservoirs underlying Arabia Terra.

Analysis of THEMIS night images shows that SLE and MLE craters display a range of preservation, indicating that the conditions under which these ejecta types form have been present for long time periods. Analysis of other crater characteristics used to indicate preservation (e.g., crater depth, rim height, superposition of subsequent craters, visual appearance, etc.) (Barlow, 2004) support this conclusion. Thus, if the MLE morphology results from excavation into liquid reservoirs, the range of MLE crater preservation suggests that an aquifer has been long-lived in this region.

2.5.2. *Central pits*

The Arabia Terra province is also unusual in the number of craters displaying central pits (Fig. 9 and Table 2). Central pits observed on Mars occur either on the crater floor or atop central rises/peaks ("summit pits"), with floor pits being slightly favored over summit pits. Central pits are proposed to form by degassing of volatile-rich target material during crater formation (Wood et al., 1978); this is supported by recent numerical modeling of impacts into ice–soil mixed targets (Pierazzo et al., 2005). Barlow and Bradley (1990) reported that central pits are distributed preferentially along the rim and possible outer rings of large impact basins and suggested that fracturing of target

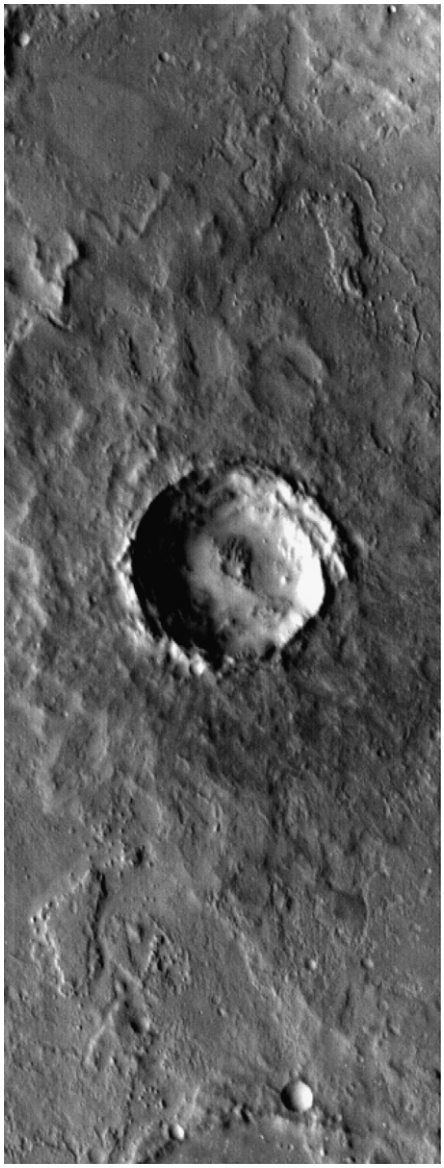

Fig. 9. Example of MLE crater containing a central pit. Crater is 16 km in diameter and located at 15.09° N, 348.64° E. Both the multiple layer ejecta pattern and the central pit are believed to be indicators of the presence of subsurface volatiles. (THEMIS image I02035009.)

Table 2
Percentage of central pit craters relative to all craters showing either a central peak or a central pit within 10° latitude by 10° longitude blocks and with the basin location shaded. Each box contains an average of 35 craters displaying either a central peak or central pit

	Pit craters						
	350–360E	0–10E	10–20E	20–30E	30–40E	40–50E	50–60E
40N–50N	50	0	33	0	0	50	0
30N–40N	23	20	38	36	50	14	50
20N–30N	27	40	22	23	31	10	21
10N–20N	65	29	28	25	17	8	42
0–10N	57	64	50	24	10	32	47
10S–0	25	100	21	75	37	30	35
20S–10S	44	40	81	63	100	48	47

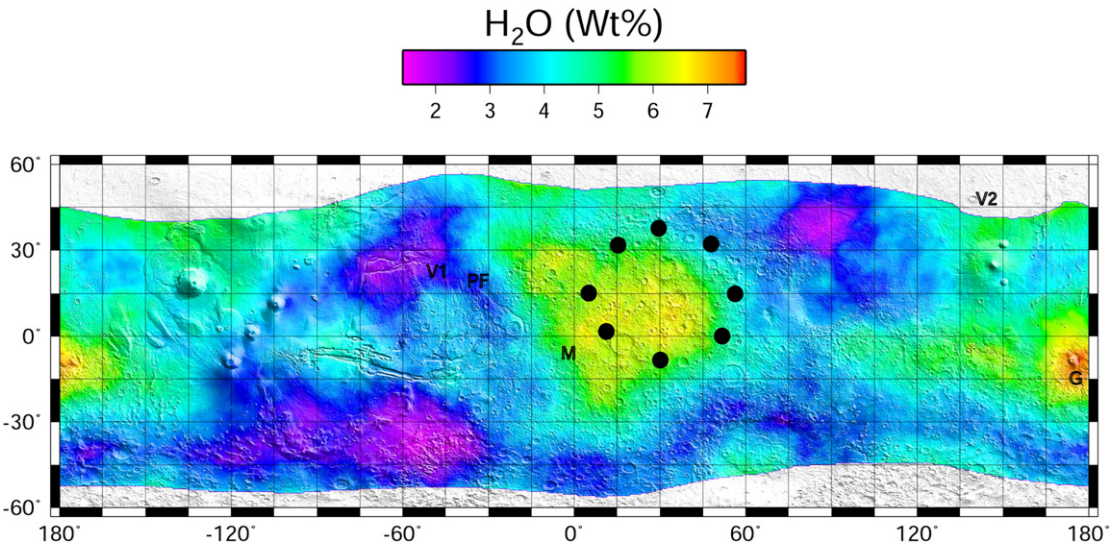

Fig. 10. Anomalous elevated hydrogen/H_2O concentration in the Arabia Terra region (e.g., Boynton et al., 2002, 2007; Feldman et al., 2002a) may mark an extremely ancient impact-derived Arabia Terra basin, including ancient sedimentary deposits such as hydrated rocks exposed from uplift and differential erosion. The H data are based on the assumption that the H is uniformly distributed with depth. If it is enriched with depth, then this is an average of low H near the surface and high H at depth (see Boynton et al., 2002, 2004). Note that the extreme NE part of the basin is not elevated in water as is the rest of the proposed primary basin, and that the area outside of the basin to the SW, W, and especially NW is equally elevated in water as the proposed primary basin. Such variation in elemental signature could be due to many factors, including thermal isostacy, structural basin adjustments, resurfacing of hydrated materials from wind and water, as well as from the Hellas impact event, and redistribution of ground water and hydrated rock materials not only related to structural adjustments, but also the hydrologic influence of the development of the highland–lowland boundary.

material during basin formation allowed volatiles to preferentially accumulate in these regions.

Central pits constitute ~25% of all interior morphologies both globally and within the 0° to 40° N latitude zone. The concentration is approximately 30% within Arabia Terra. The highest concentrations of central pits in the Arabia Terra province occur along the edge of the proposed large ancient basin and lend additional support to its formation in this region.

Approximately 35% of the central pits in Arabia Terra are found in MLE craters (Table 2) while another 25% are found in craters which no longer retain an ejecta blanket. This is consistent with results from global studies (Barlow and Hillman, 2006) which suggest that the conditions favoring formation of the MLE morphology also contribute to central pit formation. The fact that pits are seen in both fresh and degraded craters indicates that the volatiles responsible for their formation have existed in this region for much of the region's history. The relative ages of craters displaying ejecta blankets extend back to the early Hesperian/late Noachian, based on crater size-frequency distribution analysis (Barlow, 1990).

2.6. Elemental, albedo, and thermal inertia data

Arabia Terra is one of the most distinguishable parts of the planet in terms of its elemental (Boynton et al., 2002, 2004, 2007; Feldman et al., 2002a; Tokano, 2003; Fialips et al., 2005), albedo (US Geological Survey, 1991), and spectral properties [e.g., Mariner IRS (Erard and Calvin, 1997) and MGS TES (Christensen et al., 2001)]. Data from the Gamma Ray Spectrometer (GRS) aboard Mars Odyssey indicates that the Arabia Terra province has an elevated hydrogen (H) content (Fig. 10), ranging between 5 and 7 wt% equivalent water after smoothing with a mean boxcar filter with a radius of 10° (GRS detects H, not H_2O or OH; nevertheless, for uniformity throughout this paper, we report H_2O equivalent wt% computed from H concentrations; see Boynton et al. (2007) for a more detailed explanation of H_2O equivalent wt%). The average concentration of water for the Arabia region is 5.7 wt% equivalent water content, which is higher than the 3.9 wt% equivalent water content global average for non-polar regions.

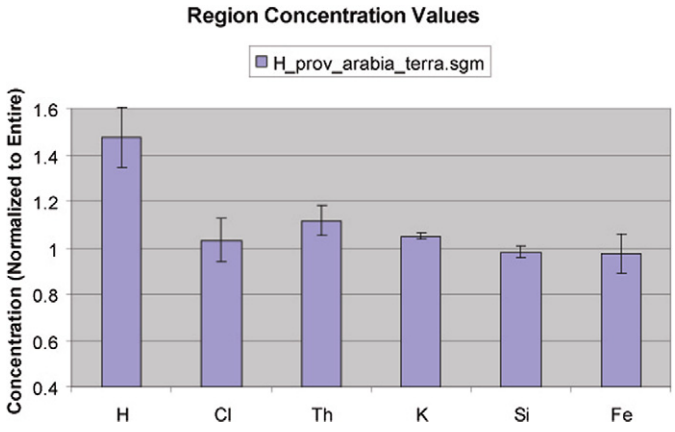

Fig. 11. Figure shows elemental enrichment factors for H, Cl, Th, K, Si, and Fe, determined using Gamma Ray sums for the Arabia Terra province. Concentration values have been normalized to the average concentration of the equatorial regions (excluding polar regions with high concentrations of water ice; for more information, see Boynton et al., 2007). Note that H, Th, and K are elevated.

Fig. 11 shows average concentration values for the six elements determined thus far using gamma ray data for both Arabia Terra and the entire planet, excluding the polar regions. These values were determined by taking an equal area average of concentration values determined for $5° \times 5°$ grids within each region shown. Also shown is the estimated error in the mean, which is affected by both instrument accuracy and variance within each region. Elements other than water do not show significant deviations from the global average in this analysis.

Hydrated minerals seem a likely candidate for explaining much of the observed H_2O equivalent wt% computed from H in Arabia Terra (Gendrin et al., 2005; Fialips et al., 2005). If this is the case, then the elevated signatures in and beyond the proposed primary basin may be due to exposure and redistribution of basin sourcing hydrated minerals by wind and other resurfacing processes. If the proposed basin is a multi-ringed impact basin, then the elemental signature would be greater in extent, as there would be structurally controlled depressions concentric about the primary basin also with such rock materials. These materials would subsequently have been resurfaced by wind and water as well as by the Hellas impact event.

The possibility of water ice accounting for some of the elevated hydrogen cannot yet be completely ruled out and a connection to a larger volatile reservoir within the proposed basin may be possible. The basin would have served as a sink for water as well as other deposits. Water would turn to ice under current climatic conditions, particularly in localized cold niches formed by topographic relief (Paige et al., 2003; Feldman et al., 2005). Jakosky and Carr (1985) argue that polar surface ice sublimates and is transported to the equator to form an ice "belt," an idea supported by recent global circulation models (GCMs). The GCMs indicate that water ice is stable at the tropics and will migrate there during periods of high obliquity (>45°) (Mischna et al., 2003). This ice is not uniformly distributed, preferentially accumulating in regions of low thermal inertia (Richardson et al., 2003). Ice deposition is expected in the Arabia Terra province since it is a region characterized by low thermal inertia. If dust accumulation slows the rate at which water returns to the poles at low obliquity, ice can be retained over time scales substantially longer than those required for its emplacement, allowing thick sequences of dust and ice to accumulate (Mischna et al., 2003). Such surface and atmospheric water interactions contribute to the long-term evolution and distribution of subsurface water and can help explain the GRS-detected hydrogen signature of the Arabia Terra province. Other contributing factors may include resurfacing from the Hellas impact (e.g., dewatering and reworking of Arabia Terra materials) and hydrologic activity resulting from the formation of the highland–lowland boundary.

In summary, an ancient Arabia Terra basin is consistent with the elevated H signature observed by GRS. We propose that layered sedimentary materials (including evaporates) were emplaced during wetter conditions (Malin and Edgett, 2000, 2001, 2003; Edgett and Malin, 2002; Baker et al., 2002) within the giant basin, eroded from diverse and far-reaching geologic provinces surrounding the basin. These wetter conditions also led to the establishment of long lasting water enrichment, perhaps in the form of regional and/or perched aquifers. The Odyssey results alone cannot indicate the depth to which this H_2O extends as it is sensitive to only the top 30 cm or so. However, the impact crater record suggests that water enrichment in the Arabia Terra region occurs at depths of at least a few kilometers even up to recent times.

2.7. Geophysical characteristics and modeling

Through the geologic approach, which includes tier-scalable reconnaissance, the geologist compiles the layers of information for comparative analysis. A significant part of this approach, which should not be overlooked if existing (in this case, thanks to the highly successful MGS mission), is evaluating the geophysical information through modeling. Such effort is particularly valid for topographic/basin reconstructions of Earth, as is done in the petroleum industry. Thus, the role of this part of the investigation is simply to investigate whether the geophysical data are consistent with the hypothesis, rather than to prove it theoretically, as it is impossible in most cases. Importantly, we present an argument for a basin, not necessarily of impact origin. The basin hypothesis is necessary because there clearly seems to be an area of sediment accumulation, history of erosional processes, volatile accumulation, etc. Though a basin of possible impact origin is modeled below, we emphasize that the proposed basin may be the result of plate tectonism in origin (e.g., Connerney et al., 2005).

2.7.1. Free-air gravity

Arabia Terra is distinct in its free-air gravity signature, which is relatively uniform when compared to other regions of the southern highlands (Fig. 12), except for the similar uniform signature surrounding Hellas. The free-air gravity over Arabia is largely devoid of large topographic and gravitational variations, aside from a general sloping to the west and northwest. There is no discernable mascon, as is commonly seen in impact basins, but a mascon would not be expected if the basin was filled with material when the lithosphere was still relatively thin

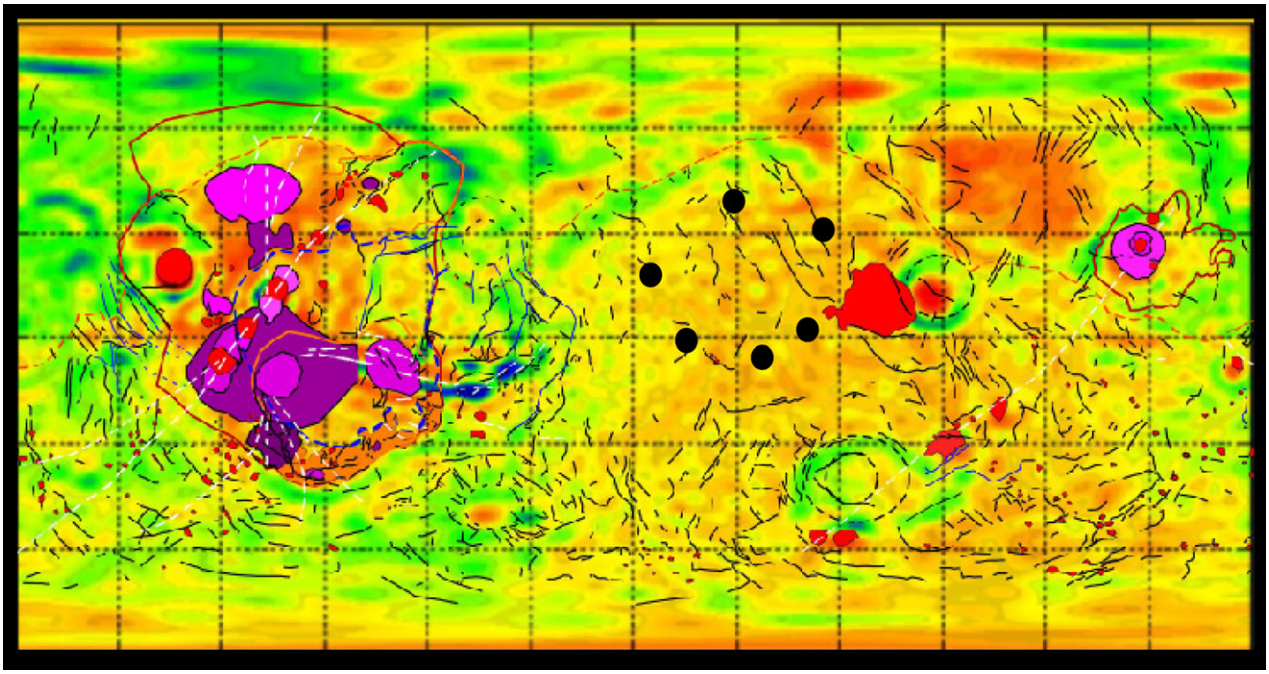

Fig. 12. Similar to Fig. 3 (including the dots that mark the location of the proposed primary ancient basin), but macrostructures superposed on free-air gravity anomalies (red is high and blue is low), which were computed from MGS75D gravity model [see Yuan et al. (2001), which includes the corresponding color scale]. Note that when compared to the rest of Mars, the broad uniform gravity signal (MGS Science Team) may mark an ancient Arabia Terra basin (e.g., extensive basin infill).

and weak early in the planet's history when heat flow was substantially higher (Solomon et al., 2005). The Arabia basin has likely undergone substantial isostatic adjustment due to its ancient age, giving rise to the uniform gravity signature. Under the conditions of a thin lithosphere (providing little elastic support), any subsequent deposition within the basin would simply cause further isostatic adjustments rather than producing a measurable gravity anomaly. Gravity and topography admittance and correlation spectra are broadly consistent with the topography being isostatically compensated with an effective elastic thickness $T_e < 16$ km (McGovern et al., 2002, 2004).

We estimate the free-air gravity anomaly that would result from filling a >1000-km-diameter basin with material of varying densities by using a model based on a spherical thin elastic shell (Fig. 13). Following the formulation of Turcotte et al. (1981) and Willemann and Turcotte (1982), we determine the vertical displacement of the lithosphere for an initial topographic configuration of the surface and Moho with a crust and mantle density of 2900 and 3500 kg m^{-3}, respectively. Following Zuber et al. (2000) and Banerdt (2004), we use MOLA-derived topography of the Hellas impact basin and the corresponding Moho topography (Neumann et al., 2004) as our starting conditions since Hellas represents a large (>1000-km-diameter) ancient basin that has remained relatively unfilled and is in near-isostatic equilibrium. The basin is then filled with material, taking into account lithospheric deflection, until the topography is flat. From the resulting configuration of the filled basin and Moho, we determine the resulting gravity anomaly assuming a mean crustal thickness of 50 km.

The resulting gravity anomaly values within the basin are plotted in Fig. 13 for a range of fill densities and effective

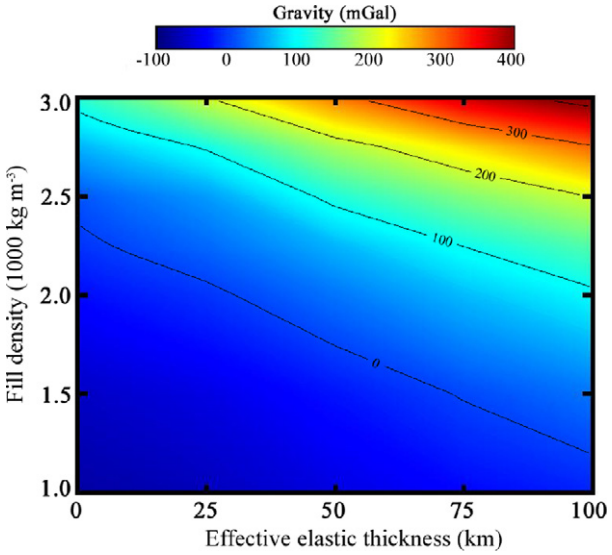

Fig. 13. The variation in gravity anomaly generated by filling Hellas basin with material of differing densities and elastic thickness values with crust thickness (50 km) and density (2900 kg m^{-3}) held constant.

elastic thicknesses. There is a trade-off between these two parameters and generally for low fill densities and elastic thicknesses (i.e., $\rho \sim 1000$–1800 kg m^{-3} and $T_e < 50$ km), the gravity anomaly is negligible or negative. At higher fill densities ($\rho > 2400$ kg m^{-3}), a mascon is produced with increasing magnitude as elastic thickness increases. As can been seen from our results, the absence of an associated mascon with the proposed basin in Arabia Terra is expected for a relatively thin T_e at the time the basin was filled. For values of $T_e < 16$ km,

determined by McGovern et al. (2004) to be appropriate for Arabia Terra, and a range of basin fill densities consistent with sediments (~2200–2400 kg m^{-3}), a gravity anomaly is not predicted. In contrast, the buried Utopia impact basin (McGill, 1989) has a broad, ~100–200 mGal mascon associated with it. The infilling material generating the Utopia mascon occurred at a later time when T_e was significantly larger. Zuber et al. (2000), Banerdt (2004), and Searls and Phillips (2004) estimate that $T_e \sim 100$ km gives the best fit to the Utopia mascon.

The absence of any geophysical manifestation of a basin in Arabia Terra in the gravity data can also result, in part, by viscous relaxation of the crater cavity. If the lithosphere is sufficiently thin when an impact occurs, the initial excavated basin will respond by rebounding due to the ductile behavior of the martian crust.

The rebound process of a large crater cavity is similar to that of postglacial rebound. In this case, the surface displacement d can be written as

$$d = d_0 e^{-t/\tau_r}, \tag{2}$$

where d_0 is the original depth of the crater and τ_r is the characteristic time for the relaxation, given by

$$\tau_r = \frac{4\eta}{\rho g D}, \tag{3}$$

where η is the viscosity of the mantle, ρ is the density of the mantle, and D is the diameter of the crater (Turcotte and Schubert, 1982). Assuming that the viscosity of the crust and the mantle in Arabia Terra early in martian history was ~10^{21}–10^{25} Pa s, the characteristic time for relaxation becomes fairly short, 10^3–10^7 years, resulting in a greatly reduced topographic expression for an ancient Arabia basin.

In summary, the ancient age of the Arabia Terra basin-forming event can explain the uniform appearance of the gravity. Factors contributing to the diminution of any geophysical signature that may have developed include (1) Arabia's proximity to the crustal dichotomy, (2) superposition of ejecta from the later Utopia, Hellas, and Isidis impacts, and (3) uplift and erosion in response to the development of Tharsis. Subsurface information from ground penetrating [e.g., possibly Mars Express (MARSIS) and Mars Reconnaissance Orbiter (SHARAD)] and seismic experiments could yield information to evaluate and test the basin hypothesis.

2.7.2. *Magnetic anomalies*

Magnetic anomalies are observed in the Arabia Terra region, although their magnitude is less pronounced than the strong anomalies in Terra Cimmeria (Acuña et al., 1999, 2001; Connerney et al., 1999, 2005; Arkani-Hamed, 2003). If the hypothesized Arabia basin is the result of a giant impact, the impact would have erased any preexisting magnetic anomalies in the crust, as is seen with the regions surrounding Hellas and Argyre. However, that assumes that the impact occurred after the internal magnetic dynamo died. If the impact occurred when the dynamo was active, the crust would reacquire magnetization. The diminished intensity of the magnetic anomalies in this region could indicate that the dynamo was active but in a waning stage. Alternately, the reduction in magnetic signals could result from deep burial of the magnetized crust by later basin infill; such infill could also contribute to the uniform gravity signature. T_e values found for Terra Cimmeria are of the same order as Arabia Terra (Zuber et al., 2000; McGovern et al., 2002), indicating that these two provinces are of comparable age. Therefore, the weaker magnetic anomalies in Arabia Terra are likely the result of buried magnetized crust. On the other hand, the magnetic signatures in the Arabia Terra province and surrounding regions have been interpreted to mark extension, resulting from plate tectonism (Connerney et al., 2005); basins on Earth form as a result of plate tectonism such as oceanic and fault/rift basins. A giant impact occurring at a time when Mars was undergoing plate tectonism and/or creating a zone of weakness in the lithosphere for plate tectonism to exploit, however, cannot be ruled out.

3. Discussion

Ancient geologic provinces on Mars not destroyed by endogenic and exogenic activity following the shut down of the magnetosphere, such as the development of Tharsis (Dohm et al., 2001b) and giant impacts, including Argyre (Scott and Tanaka, 1986) and Hellas (Greeley and Guest, 1987), respectively, are revealed by stratigraphy and crater retention ages (e.g., Scott and Tanaka, 1986), as well as magnetic data (Acuña et al., 1999, 2001; Arkani-Hamed, 2003). One such window into the ancient past occurs northwest of the Hellas impact basin in Arabia Terra. Numerous characteristics described in detail in previous sections make Arabia Terra a distinctive province of Mars. The characteristics can be summarized as follows:

- the lowest topography of the heavily cratered highlands, except for the interiors of impact basins;
- predominately Noachian materials;
- a highland–lowland boundary region distinct from other boundary regions;
- the presence of very few macrostructures when compared to the rest of the cratered highlands;
- the largest and best-developed region of fretted terrain on the planet;
- outflow channels with no obvious origins;
- higher albedo and lower thermal inertia than its surroundings;
- uniform free-air gravity, compared to the rest of the highlands;
- weak remnant magnetic anomalies;
- higher H_2O and Cl signatures than the surroundings.

We interpret these to collectively indicate a possible ancient giant basin of either impact or paleotectonic origin that later became an important aquifer. If impact, the diameter of the primary basin is estimated to be at least 3000 km across based from the albedo map of the US Geological Survey (1991). Because of its ancient age, the proposed basin is not directly observed using topography. As such, this investigation is likened to those performed by terrestrial geologists to reconstruct an-

cient topographies with the exception that we are limited to remote investigation. Based on our investigation, an ancient basin in the Arabia Terra province has emerged as the most probable progenitor to explain the diverse array of characteristics. Importantly, instead of invoking a host of different processes and conditions for each characteristic, which is beyond the scope of this work, this hypothesis provides a consistent framework for describing a wide variety of characteristics, hopefully provoking further scientific inquiry.

3.1. Basin formation

The immense age of the basin is indicated by uniform free air gravity data (suggesting formation during a time of thin lithosphere and high heat flow), weak magnetic signatures, crater size-frequency distribution analysis, and the profusion of exposed materials of Noachian age. The probability of near-surface volatiles composing part of the matrix of the infilling material and continuing to be part of the subsurface composition in recent times is indicated by the exposed layered deposits, concentration of layered ejecta craters, and abundance of central pit craters.

Impact may be a viable explanation for the origin of the approximately 3000-km-diameter basin since there are impact basins of comparable size and age that occur on the Moon and Mercury. On the Moon, these include the 3600-km-diameter Procellarum basin (Whitaker, 1981; Feldman et al., 2004), an unnamed ∼3000-km-diameter basin on the lunar farside (Feldman et al., 2002b), and the 2500-km-diameter South Pole–Aitken basin. While only 25% of Mercury has been observed at Sun angles sufficient to detect basins with a faint topographic signature, such analysis has revealed the old 1500-km-diameter Borealis Basin. All of these basins are heavily cratered and highly degraded, indicating their ancient formational age.

The timing of the Arabia Terra basin-forming event is difficult to determine other than saying it is ancient. Mars formed out of the solar nebula about 4.5×10^9 years ago and its lithosphere likely became thick enough to retain impact scars within a few million years after that. The lack of a free-air gravity anomaly and the relatively weak magnetic signatures in this area indicate that the event forming the Arabia Terra basin occurred when the lithosphere was thin and prior to the shutdown of the magnetic dynamo (Arkani-Hamed, 2004). More recent basin-forming impacts, such as Argyre and Hellas, demagnetized the surrounding crust, so if the Arabia basin is due to an impact it must have occurred earlier than Argyre and Hellas. Crater statistical studies and stratigraphic analysis indicates that Argyre and Hellas formed during the Late Heavy Bombardment (LHB) period (e.g., Barlow, 1988), which, based on analysis of lunar samples, ended about 3.8 Gyr on the Moon (Stöffler and Ryder, 2001). While some argue that gigantic impacts occurred throughout the LHB period (Hartmann, 2003), there is growing evidence that this period was a catastrophic event that occurred in only an ∼10 to ∼150 Myr long time period (Gomes et al., 2005; Tsiganis et al., 2005; Kring and Cohen, 2002; Strom et al., 2005). This means that the heavily cratered terrain on Mars dating from the LHB may range from ∼3.9 to 3.8 Gyr old. The objects responsible for causing the LHB were largely derived from the main asteroid belt (Strom et al., 2005), although there could have been a massive bombardment of cometary planetisimals during the first 30 Myr of the LHB (Gomes et al., 2005). If the LHB was a catastrophic event, it surely would have destroyed most if not all of the cratering record that was present before that time.

The degraded nature of the Arabia Terra basin indicates it formed either before or at the very beginning of the LHB. If the LHB was a catastrophic event, the Arabia basin is likely no older than 3.95 Gyr. If the LHB was not a catastrophic event or it did not completely destroy the pre-existing cratering record, the Arabia Basin is likely older than 4.0 Gyr.

3.2. History of the Arabia Terra region

Combining the information presented in the preceding sections, we propose the following sequence of events in the Arabia Terra region:

(1) An enormous basin, possibly of impact origin, forms early in martian history. The lack of a free-air gravity anomaly suggests that the lithosphere was thin at the time of basin formation. The remnant crustal magnetic anomalies indicate that the magnetic dynamo was still active. Those observations combined with the Noachian materials within the basin and the very degraded nature of the basin itself suggest the ancient age of this event.
(2) Sediments and other materials are deposited within the basin during an early period of high erosion rates. Crater analysis indicates that these materials were emplaced during the Noachian Period. The sediments become enriched with water through runoff, ponding, and infiltration.
(3) The thin lithosphere led to rapid isostatic adjustment of the basin and its superposed materials.
(4) Tharsis began to grow on the opposite side of the planet. This caused the antipodal bulge in Arabia Terra to form leading to differential erosion within the basin and exposing the stratigraphic sequences initially deposited in the basin.
(5) Impact cratering, fluvial erosion, and other geologic processes have reworked the basin material over the subsequent ∼4.0 Gyr. The ejecta morphologies and central pits associated with many impact craters in this area indicate that parts of the basin remain water-enriched up to the present day.

4. Implications

A hypothesized ancient basin, possibly of impact origin, in the Arabia Terra province and its associated water-enriched sediments helps to explain a number of unique characteristics of this region. The establishment of such an ancient basin would lead to long-term water enrichment in this region. Could the basin hypothesis help explain the reported elevated methane in the atmosphere above the Arabia Terra region, as the region is one of only three locations on Mars where elevated

concentrations of methane have been identified. Interpretations include biological, hydrothermal, and release of methane clathrates (Mumma et al., 2004; Atreya et al., 2004; Formisano et al., 2004; Allen and Oehler, 2005; Oehler et al., 2005; Prieto-Ballesteros et al., 2006)?

The existence of an ancient, ~3000-km-diameter basin in Arabia Terra, taken in conjunction with other large, buried impact basins such as the Chryse and putative Tharsis basins (Dohm et al., 2001b, 2001c), suggests that rapid obscuration of basins and infill with volatile-rich materials was a relatively common phenomena early in martian history. This has profound implications for rates of deposition in the earliest recorded part of martian history and suggests an environment with vigorous geomorphic processes being driven by a dynamic hydrosphere. The proposed Arabia Terra basin also constrains the formation period of the northern lowlands. Although our evidence suggests that the lowlands postdate the formation and infilling of the Arabia Terra basin, several investigators have suggested that the dichotomy was shaped by early geophysical phenomena, such as mantle convection associated with core formation (Wise et al., 1979; Zuber et al., 2000). If so, why were the northern lowlands not also infilled by materials and therefore obscured to the present day? Were rates of deposition somehow different for the polar regions and/or was the temporal extent of the mechanism that formed the northern plains and global dichotomy greater, perhaps related to incipient plate tectonics (Maruyama et al., 2001; Baker et al., 2002; Dohm et al., 2002; Fairén et al., 2002; Fairén and Dohm, 2004)? Although many questions remain to be answered, the emerging picture is that the topography of earliest Mars was drastically different from what is observed today. This topography was dominated by large basins, many if not all formed by impact (Frey et al., 2002, 2003, 2005). Volatile-rich materials preferentially accumulated in these depressions, giving rise to many of the characteristics observed in areas such as Arabia Terra. Such huge basins also may have excavated large amounts of mantle rock. Identification of such mantle rocks would be very difficult at the present time since they are undoubtedly mixed with crustal rocks, altered by later aqueous processes, and partly covered by subsequent deposits such as volcanic flows. However, these mantle rocks would be extremely valuable in understanding the bulk composition of Mars at the time of their excavation. Thus, exploration of ancient basins such as the proposed Arabia Terra basin will provide important new insights into the early history, internal and surface evolution, and astrobiological potential of Mars.

Acknowledgments

We are grateful to Leslie F. Bleamaster III and Robert R. Herrick for their thoughtful reviews, both of which resulted in a significantly improved manuscript.

References

Acuña, M.H., Connerney, J.E.P., Ness, N.F., Lin, R.P., Mitchell, D., Carlson, C.W., McFadden, J., Anderson, K.A., Reme, H., Mazelle, C., Vignes, D., Wasilewski, P., Cloutier, P., 1999. Global distribution of crustal magnetization discovered by the Mars Global Surveyor MAG/ER experiment. Science 284, 790–793.

Acuña, M.H., Connerney, J.E.P., Wasilewski, P., Lin, R.P., Mitchell, D., Anderson, K.A., Carlson, C.W., McFadden, J., Réme, H., Mazelle, C., Vignes, D., Bauer, S.J., Cloutier, P., Ness, N.F., 2001. Magnetic field of Mars: Summary of results from the aerobraking and mapping orbits. J. Geophys. Res. 106, 23403–23417.

Allen, C.C., Oehler, D.Z., 2005. Thinking like a wildcatter—Prospecting for methane in Arabia Terra, Mars. Lunar Planet. Sci. XXXVI. Abstract 1398 [CD-ROM].

Anderson, R.C., Dohm, J.M., Golombek, M.P., Haldemann, A., Franklin, B.J., Tanaka, K.L., Lias, J., Peer, B., 2001. Significant centers of tectonic activity through time for the western hemisphere of Mars. J. Geophys. Res. 106, 20563–20585.

Anderson, R.C., Dohm, J.M., Haldemann, A.F.C., Pounders, E., Golombek, M., Castano, A., 2006. Centers of tectonic activity for the eastern hemisphere. Icarus, submitted for publication.

Arkani-Hamed, J., 2003. Thermoremanent magnetization of the martian lithosphere. J. Geophys. Res. 108, doi:10.1029/2003JE002049.

Arkani-Hamed, J., 2004. Timing of the martian core dynamo. J. Geophys. Res. 109, doi:10.1029/2003JE002195.

Atreya, S., Encrenaz, T., Formisano, V., Wong, A.S., 2004. Methane on Mars—Sources, sinks, and implications for life. In: Abstracts of the Int. Mars Conf., Ischia Island, Sept. 19–23.

Baker, V.R., Maruyama, S., Dohm, J.M., 2002. A theory of plate tectonics and subsequent long-term superplume activity on Mars. In: International Workshop: Role of superplumes in the Earth System. Electron. Geosci. 7, 312–316.

Banerdt, W.B., 2004. A gravity analysis of the subsurface structure of the Utopia impact basin. Lunar Planet. Sci. XXXV. Abstract 2043 [CD-ROM].

Barlow, N.G., 1988. Crater size-frequency distributions and a revised martian relative chronology. Icarus 75, 285–305.

Barlow, N.G., 1990. Constraints on early events in martian history as derived from the cratering record. J. Geophys. Res. 95, 14191–14201.

Barlow, N.G., 2004. Martian subsurface volatile concentrations as a function of time: Clues from layered ejecta craters. Geophys. Res. Lett. 31, doi:10.1029/2003GL019075.

Barlow, N.G., 2005a. Martian impact craters as revealed by MGS and Odyssey. Lunar Planet. Sci. XXXVI. Abstract 1415.

Barlow, N.G., 2005b. A review of martian impact crater ejecta structures and their implications for target properties. In: Kenkmann, T., Hörz, F., Deutsch, A. (Eds.), Large Meteorite Impacts III, Geol. Soc. Am. Spec. Paper 384, pp. 433–442.

Barlow, N.G., Bradley, T.L., 1990. Martian impact craters: Correlations of ejecta and interior morphologies with diameter, latitude, and terrain. Icarus 87, 156–179.

Barlow, N.G., Hillman, E., 2006. Distributions and characteristics of martian central pit craters. Lunar Planet. Sci. XXXVII. Abstract 1253.

Barlow, N.G., Perez, C.B., 2003. Martian impact crater ejecta morphologies as indicators of the distribution of subsurface volatiles. J. Geophys. Res. 108, doi:10.1029/2002JE002036.

Barlow, N.G., Boyce, J.M., Costard, F.M., Craddock, R.A., Garvin, J.B., Sakimoto, S.E.H., Kuzmin, R.O., Roddy, D.J., Soderblom, L.A., 2000. Standardizing the nomenclature of martian impact crater ejecta morphologies. J. Geophys. Res. 105, 26733–26738.

Barlow, N.G., Koroshetz, J., Dohm, J.M., 2001. Variations in the onset diameter for martian layered ejecta morphologies and their implications for subsurface volatile reservoirs. Geophys. Res. Lett. 28, 3095–3098.

Barnouin-Jha, O.S., Schultz, P.H., Lever, J.H., 1999a. Investigating the interactions between an atmosphere and an ejecta curtain. 1. Wind tunnel tests. J. Geophys. Res. 104, 27105–27115.

Barnouin-Jha, O.S., Schultz, P.H., Lever, J.H., 1999b. Investigating the interactions between an atmosphere and an ejecta curtain. 2. Numerical experiments. J. Geophys. Res. 104, 27117–27131.

Barosio, A.H., Valdés-Galicia, J.F., Urrutia-Fucugauchi, J., 2002. Mars thermal history based on its tectonic and structural systems. Geofís. Int. 41, 189–193.

Boynton, W.V., Feldman, W.C., Squyres, S.W., Prettyman, T., Brückner, J., Evans, L.G., Reedy, R.C., Starr, R., Arnold, J.R., Drake, D.M., Englert, P.A.J., Metzger, A.E., Mitrofanov, I., Trombka, J.I., d'Uston, C., Wänke, H., Gasnault, O., Hamara, D.K., Janes, D.M., Marcialis, R.L., Maurice, S., Mikheeva, I., Taylor, G.J., Tokar, R., Shinohara, C., 2002. Distribution of hydrogen in the near-surface of Mars: Evidence for subsurface ice deposits. Science 297, 81–85.

Boynton, W.V., Feldman, W.C., Mitrofanov, I., Evans, L.G., Reedy, R.C., Squyres, S.W., Starr, R., Trombka, J.I., d'Uston, C., Arnold, J.R., Englert, P.A.J., Metzger, A.E., Wänke, H., Brückner, J., Drake, D.M., Shinohara, C., Fellows, C., Hamara, D.K., Harshman, K., Kerry, K., Turner, C., Ward, M., Barthe, H., Fuller, K.R., Storms, S.A., Thornton, G.W., Longmire, J.L., Litvak, M.L., Ton'Chev, A.K., 2004. The Mars Odyssey Gamma-Ray Spectrometer instrument suite. Space Sci. Rev. 110, 37–83.

Boynton, W.V., and 26 colleagues, 2007. Distribution of Common Elements on the Surface of Mars as determined by the 2001 Mars Odyssey Gamma-Ray Spectrometer: Maps and data reduction methods. J. Geophys. Res., submitted for publication.

Carr, M., 2001. Mars Global Surveyor observations of martian fretted terrain. J. Geophys. Res. 106, 23571–23594.

Carr, M.H., Crumpler, L.S., Cutts, J.A., Greeley, R., Guest, J.E., Masursky, H., 1977. Martian impact craters and emplacement by surface flow. J. Geophys. Res. 82, 4055–4065.

Christensen, P.R., Bandfield, J.L., Hamilton, V.E., Ruff, S.W., Kieffer, H.H., Titus, T.N., Malin, M.C., Morris, R.V., Lane, M.D., Clark, R.L., Jakosky, B.M., Mellon, M.T., Pearl, J.C., Conrath, B.J., Smith, M.D., Clancy, R.T., Kuzmin, R.O., Roush, T., Mehall, G.L., Gorelick, N., Bender, K., Murray, K., Dason, S., Greene, E., Silverman, S., Greenfield, M., 2001. The Mars Global Surveyor Thermal Emission Spectrometer experiment: Investigation description and surface science results. J. Geophys. Res. 106, 23823–23871.

Connerney, J.E.P., Acuña, M.H., Wasilewski, P.J., Kletetschka, G., Ness, N.F., Rème, H., Lin, R.P., Mitchell, D.L., 1999. The global magnetic field of Mars and implications for crustal evolution. Science 284, 790–793.

Connerney, J.E.P., Acuña, M.H., Ness, N.F., Kletetschka, G., Mitchell, D.L., Lin, R.P., Reme, H., 2005. Tectonic implications of Mars crustal magnetism. Proc. Nat. Acad. Sci. USA 102, 14970–14975.

Costard, F.M., 1989. The spatial distribution of volatiles in the martian hydrolithosphere. Earth Moon Planets 45, 265–290.

Crown, D.A., Price, K.H., Greeley, R., 1992. Geologic evolution of the east rim of the Hellas basin, Mars. Icarus 100, 1–25.

Dohm, J.M., Tanaka, K.L., Hare, T.M., 2001a. Geologic map of the Thaumasia region of Mars. USGS Misc. Inv. Ser. Map I-2650, scale 1:5,000,000.

Dohm, J.M., Ferris, J.C., Baker, V.R., Anderson, R.C., Hare, T.M., Strom, R.G., Barlow, N.G., Tanaka, K.L., Klemaszewski, J.E., Scott, D.H., 2001b. Ancient drainage basin of the Tharsis region, Mars: Potential source for outflow channel systems and putative oceans or paleolakes. J. Geophys. Res. 106, 32943–32958.

Dohm, J.M., Anderson, R.C., Baker, V.R., Ferris, J.C., Rudd, L.P., Hare, T.M., Rice Jr., J.W., Casavant, R.R., Strom, R.G., Zimbelman, J.R., Scott, D.H., 2001c. Latent outflow activity for western Tharsis, Mars: Significant flood record exposed. J. Geophys. Res. 106, 12301–12314.

Dohm, J.M., Maruyama, S., Baker, V.R., Anderson, R.C., Ferris, J.C., Hare, T.M., 2002. Plate tectonism on early Mars: Diverse geological and geophysical evidence. Lunar Planet. Sci. XXXIII. Abstract 1639 [CD-ROM].

Dohm, J.M., Ferris, J.C., Barlow, N.G., Baker, V.R., Mahaney, W.C., Anderson, R.C., Hare, T.M., 2004. The Northwestern Slope Valleys (NSVs) region, Mars: A prime candidate site for the future exploration of Mars. Planet. Space Sci. 52, 189–198.

Dohm, J.M., Kerry, K., Keller, J.M., Baker, V.R., Maruyama, S., Anderson, R.C., Ferris, J.C., Hare, T.M., 2005. Mars geological province designations for the interpretation of GRS data. Lunar Planet. Sci. XXXVI. Abstract 1567 [CD-ROM].

Edgett, K.S., 2005. The sedimentary rocks of Sinus Meridiani: Five key observations from data acquired by the Mars Global Surveyor and Mars Odyssey orbiters. Mars 1, 5–58.

Edgett, K.S., Malin, M.C., 2002. Martian sedimentary rock stratigraphy: Outcrops and interbedded craters of northwest Sinus Meridiani and southwest Arabia Terra. Geophys. Res. Lett. 29, doi:10.1029/2002GL016515.

Erard, S., Calvin, W., 1997. New composite spectra of Mars, 0.4–5.7 μm. Icarus 130, 449–460.

Fairén, A.G., Dohm, J.M., 2004. Age and origin of the lowlands of Mars. Icarus 168, 277–284.

Fairén, A.G., Ruiz, J., Anguita, F., 2002. An origin for the linear magnetic anomalies on Mars through accretion of terranes: Implications for dynamo timing. Icarus 160, 220–223.

Fairén, A.G., Dohm, J.M., Baker, V.R., de Pablo, M.A., Ruiz, J., Ferris, J.C., Anderson, R.C., 2003. Episodic flood inundations of the northern plains of Mars. Icarus 165, 53–67.

Fairén, A.G., Fernández-Remolar, D., Dohm, J.M., Baker, V.R., Amils, R., 2004. Inhibition of carbonate synthesis in acidic oceans on early Mars. Nature 431, 423–426.

Feldman, W.C., Boynton, W.V., Tokar, R.L., Prettyman, T.H., Gasnault, O., Squyres, S.W., Elphic, R.C., Lawrence, D.J., Lawson, S.L., Maurice, S., McKinney, G.W., Moore, K.R., Reedy, R.C., 2002a. Global distribution of neutrons from Mars: Results from Mars Odyssey. Science 297, 75–78.

Feldman, W.C., Gasnault, O., Maurice, S., Lawrence, D.J., Elphic, R.C., Lucey, P.C., Binder, A.B., 2002b. Global distribution of lunar composition: New results from Lunar Prospector. J. Geophys. Res. 107 (E3), doi:10.1029/2001JE001506.

Feldman, W.C., Ahola, K., Barraclough, B.L., Belian, R.D., Black, R.K., Elphic, R.C., Everett, D.T., Fuller, K.R., Kroesche, J., Lawrence, D.J., Lawson, S.L., Longmire, J.L., Maurice, S., Miller, M.C., Prettyman, T.H., Storms, S.A., Thornton, G.W., 2004. Gamma-ray, neutron, and alpha-particle spectrometers for the Lunar Prospector mission. J. Geophys. Res. 109, doi:10.1029/2003JE002207.

Feldman, W.C., Prettyman, T.H., Maurice, S., Nelli, S., Elphic, R., Funsten, H.O., Gasnault, O., Lawrence, D.J., Murphy, J.R., Tokar, R.L., Vaniman, D.T., 2005. Topographic control of hydrogen deposits at lowlatitudes to midlatitudes of Mars. J. Geophys. Res. 110, doi:10.1029/2005JE002452.

Fialips, C.I., Carey, J.W., Vaniman, D.T., Bish, D.L., Feldman, W.C., Mellon, M.T., 2005. Hydration state of zeolites, clays, and hydrated salts under present-day martian surface conditions: Can hydrous minerals account for Mars Odyssey observations of near-equatorial water-equivalent hydrogen? Icarus 178, 74–83.

Formisano, V., Atreya, S., Encrenaz, T., Ignatiev, N., Giuranna, M., 2004. Detection of methane in the atmosphere of Mars. Science 306, 1758–1761.

Frey, H.V., Roark, J.H., Shockey, K.M., Frey, E.L., Sakimoto, S.E.H., 2002. Ancient lowlands on Mars. Geophys. Res. Lett. 29, doi:10.1029/2001GL013832.

Frey, H.V., Frey, E.L., Hartmann, W.K., Tanaka, K.L., 2003. Evidence for buried "pre-Noachian" crust pre-dating the oldest observed surface units on Mars. Lunar Planet. Sci. XXXIV. Abstract 1848 [CD-ROM].

Frey, H.V., DeSoto, G.E., Lazrus, R.M., 2005. Regional studies of highland–lowland age differences across the Mars crustal dichotomy boundary. Lunar Planet. Sci. XXXVI. Abstract 1407 [CD-ROM].

Garvin, J.B., Sakimoto, S.E.H., Frawley, J.J., Schnetzler, C., 2000. North polar region craterforms on Mars: Geometric characteristics from the Mars Orbiter Laser Altimeter. Icarus 144, 329–352.

Gendrin, A., Mangold, N., Bibring, J.P., Langevin, Y., Gondet, B., Poulet, F., Bonello, G., Quantin, C., Mustard, J., Arvidson, R., LeMouelic, S., 2005. Sulfates in martian layered terrains: The OMEGA/Mars Express view. Science 307, 1587–1591.

Golombek, M.P., Plescia, J.B., Franklin, B.J., 1991. Faulting and folding in the formation of planetary wrinkle ridges. Proc. Lunar Sci. Conf. 21, 679–693. Abstract.

Gomes, R., Levison, H.F., Tsiganis, K., Morbidelli, A., 2005. Origin of the Cataclysmic Late Heavy Bombardment period of the terrestrial planets. Nature 435, 466–469.

Greeley, R., Guest, J.E., 1987. Geologic map of the eastern equatorial region of Mars. USGS Misc. Inv. Ser. Map I-1802B (1:15,000,000).

Hartmann, W.K., 2003. Megaregolith evolution and cratering cataclysm models—Lunar cataclysm as a misconception (28 years later). Meteor. Planet. Sci. 38, 579–593.

Head, J.W., Pratt, S., 2001. Extensive Hesperian-aged south polar ice sheet on Mars: Evidence for massive melting and retreat, and lateral flow and ponding of meltwater. J. Geophys. Res. 106, 12275–12299.

Hynek, B.M., Phillips, R.J., 2001. Evidence for extensive denundation of the martian highlands. Geology 29, 407–410.

Jakosky, B.M., Carr, M.H., 1985. Possible precipitation of ice at low latitudes of Mars during periods of high obliquity. Nature 315, 559–561.

Kargel, J.S., Strom, R.G., 1992. Ancient glaciation on Mars. Geology 20, 3–7.

Kring, D.A., Cohen, B.A., 2002. Cataclysmic bombardment throughout the inner Solar System. J. Geophys. Res. 107, doi:10.1029/2001JE001529.

Malin, M.C., Edgett, K.S., 2000. Sedimentary rocks of early Mars. Science 290, 1927–1937.

Malin, M.C., Edgett, K.S., 2001. Mars Global Surveyor Mars Orbiter Camera: Interplanetary cruise through primary mission. J. Geophys. Res. 106 (E10), 23429–23570.

Malin, M.C., Edgett, K.S., 2003. Evidence for persistent flow and aqueous sedimentation on early Mars. Science 302, 1931–1934.

Maruyama, S., Dohm, J.M., Baker, V.R., 2001. Mars plate tectonics (1): An Earth prospective. In: Am. Geophys. Union Abstracts with Programs, 82 (47), F713.

McGill, G.E., 1989. Buried topography of Utopia, Mars: Persistence of a giant impact depression. J. Geophys. Res. 94, 2753–2759.

McGill, G.E., 2002. Geologic map transecting the highland/lowland boundary zone, Arabia Terra, Mars: Quadrangles 30332, 35332, 40332, and 45332. USGS Misc. Inv. Ser. Map I-2746, scale 1:1,000,000.

McGovern, P.J., Solomon, S.C., Smith, D.E., Zuber, M.T., Simons, M., Wieczorek, M.A., Phillips, R.J., Neumann, G.A., Aharonson, O., Head, J.W., 2002. Localized gravity/topography admittance and correlation spectra on Mars: Implications for regional and global evolution. J. Geophys. Res. 107 (E12), doi:10.1029/2002JE001854. 5136.

McGovern, P.J., Solomon, S.C., Smith, D.E., Zuber, M.T., Simons, M., Wieczorek, M.A., Phillips, R.J., Neumann, G.A., Aharonson, O., Head, J.W., 2004. Correction to "Localized gravity/topography admittance and correlation spectra on Mars: Implications for regional and global evolution." J. Geophys. Res. 109, doi:10.1029/2004JE002286. E07007.

Mischna, M.A., Richardson, M.I., Wilson, R.J., McCleese, D.J., 2003. On the orbital forcing of martian water and CO_2 cycles: A general circulation model study with simplified volatile schemes. J. Geophys. Res. 108, doi:10.1029/2003JE002051.

Moore, J.M., Wilhelms, D.E., 2001. Hellas as a possible site of ancient ice-covered lakes on Mars. Icarus 154, 258–276.

Mouginis-Mark, P., 1979. Martian fluidized ejecta morphology: Variations with crater size, latitude, altitude, and target material. J. Geophys. Res. 84, 8011–8022.

Mouginis-Mark, P.J., 1987. Water or ice in the martian regolith? Clues from rampart craters seen at very high resolution. Icarus 71, 268–286.

Mumma, M.J., Novak, R.E., DiSanti, M.A., Bonev, B.P., Dello Russo, N., 2004. Detection and mapping of methane and water on Mars. Bull. Am. Astron. Soc. 36, 1127.

Neumann, G.A., Zuber, M.T., Wieczorek, M.A., McGovern, P.J., Lemoine, F.G., Smith, D.E., 2004. Crustal structure of Mars from gravity and topography. J. Geophys. Res. 109, doi:10.1029/2004JE002262. E08002.

Oehler, D.Z., Allen, C.C., McKay, D.S., 2005. Impact metamorphism of subsurface organic matter on Mars: A potential source for Methane and surface alteration, Mars. Lunar Planet. Sci. XXXVI. Abstract 1025 [CD-ROM].

Paige, D.A., Hock, A.N., Scherbenski, J.M., Williams, J.P., 2003. Searching for ground ice at the martian equator. Eos (Fall Suppl.) 84 (46). Abstract C21C-0831.

Phillips, R.J., Zuber, M.T., Solomon, S.C., Golombek, M.P., Jakosky, B.M., Banerdt, W.B., Smith, D.E., Williams, R.M.E., Hynek, B.M., Aharonson, O., Hauck, S.A., 2001. Ancient geodynamics and global change hydrology on Mars. Science 291, 2587–2591.

Pierazzo, E., Artemieva, N.A., Ivanov, B.A., 2005. Starting conditions for hydrothermal systems underneath martian craters: Hydrocode modeling. In: Kenkmann, T., Hörz, F., Deutsch, A. (Eds.), Large Meteorite Impacts III, Geol. Soc. of America Special Paper 384, pp. 443–457.

Plescia, J.B., Golombek, M.P., 1986. Origin of planetary wrinkle ridges based on the study of terrestrial analogs. Geol. Soc. Am. Bull. 97, 1289–1299.

Prieto-Ballesteros, O., Kargel, J.S., Fairén, A.G., Fernández-Remolar, D.C., Dohm, J.M., Amils, R., 2006. Interglacial clathrate destabilization on Mars: Possible contributing source of its atmospheric methane. Geology 4, 49–152.

Richardson, M.I., Mischna, M.A., McCleese, D.J., Wilson, R.J., Vasavada, A.R., 2003. Formation of obliquity-driven subsurface ice deposits on Mars: Study with a general circulation model. Eos (Fall Suppl.) 84 (46). Abstract C12C-01.

Rodriguez, J.A.P., Saski, S., Kuzmin, R.O., Dohm, J.M., Tanaka, K.L., Miyamoto, H., Kurita, K., Komatsu, G., Fairén, A.G., Ferris, J.C., 2005a. Outflow channel sources, reactivation, and chaos formation, Xanthe Terra, Mars. Icarus 175, 36–57.

Rodriguez, J.A.P., Saski, S., Dohm, J.M., Tanaka, K.L., Strom, R., Kargel, J., Kuzmin, R.O., Miyamoto, H., Spray, J.G., Fairén, A.G., Komatsu, G., Kurita, K., Baker, V.R., 2005b. Control of impact crater fracture systems on subsurface hydrology, ground subsidence, and collapse, Mars. J. Geophys. Res. 110, doi:10.1029/2004JE002365.

Ruiz, J., Fairén, A.G., Dohm, J.M., Tejero, R., 2004. Thermal isostacy and deformation of possible paleoshorelines on Mars. Planet. Space Sci. 52, 1297–1301.

Schultz, P.H., 1992. Atmospheric effects on ejecta emplacement. J. Geophys. Res. 97, 11623–11662.

Schultz, P.H., Gault, D.E., 1979. Atmospheric effects on martian ejecta emplacement. J. Geophys. Res. 84, 7669–7687.

Scott, D.H., Tanaka, K.L., 1986. Geologic map of the western hemisphere of Mars. USGS Misc. Inv. Ser. Map I-1802-A (1:15,000,000).

Scott, D.H., Dohm, J.M., Rice Jr., J.W. 1995. Map of Mars showing channels and possible paleolake basins. USGS Misc. Inv. Ser. Map I-2461 (1:30,000,000).

Searls, M.L., Phillips, R.J., 2004. Mechanics of Utopia basin on Mars. Lunar Planet. Sci. XXXV. Abstract 1822 [CD-ROM].

Sharp, R.P., 1973. Mars: Fretted and chaotic terrains. J. Geophys. Res. 78, 4073–4083.

Sharp, R.P., Malin, M.C., 1975. Channels on Mars. Geol. Soc. Am. Bull. 86, 593–609.

Smith, D.E., Zuber, M.T., Frey, H.V., Garvin, J.B., Head, J.W., Muhleman, D.O., Pettengill, G.H., Phillips, R.J., Solomon, S.C., Zwally, H.J., Banerdt, W.B., Duxbury, T.C., Golombek, M.P., Lemoine, F.G., Neumann, G.A., Rowlands, D.D., Aharonson, O., Ford, P.G., Ivanov, A.B., Johnson, C.L., McGovern, P.J., Abshire, J.B., Afzal, R.S., Sun, X., 2001. Mars Orbiter Laser Altimeter: Experimental summary after the first year of global mapping of Mars. J. Geophys. Res. 106, 23689–23722.

Solomon, S.C., Aharonson, O., Aurnou, J.M., Banerdt, W.B., Carr, M.H., Dombard, A.J., Frey, H.V., Golombek, M.P., Hauck, S.A., Head, J.W., Jakosky, B.M., Johnson, C.L., McGovern, P.J., Neumann, G.A., Phillips, R.J., Smith, D.E., Zuber, M.T., 2005. New perspectives on ancient Mars. Science 307, 1214–1220.

Squyres, S.W., Grotzinger, J.P., Arvidson, R.E., Bell III, J.F., Calvin, W., Christensen, P.R., Clark, B.C., Crisp, J.A., Farrand, W.H., Herkenhoff, K.E., Johnson, J.R., Klingelhofer, G., Knoll, A.H., McLennan, S.M., McSween Jr., H.Y., Morris, R.V., Rice Jr., J.W., Rieder, R., Soderblom, L.A., 2004. In situ evidence for an ancient aqueous environment at Meridiani Planum, Mars. Science 306, 1709–1714.

Stewart, S.T., O'Keefe, J.D., Ahrens, T.J., 2001. The relationship between rampart crater morphologies and the amount of subsurface ice. Lunar Planet. Sci. XXXII. Abstract 2092 [CD-Rom].

Stöffler, D., Ryder, G., 2001. Stratigraphy and isotope ages of lunar geologic units: Chronological standard for the inner Solar System. Space Sci. Rev. 96, 9–54.

Strom, R.G., Malhotra, R., Ito, T., Yoshida, F., Kring, D.A., 2005. The origin of planetary impactors in the inner Solar System. Science 309, 1847–1880.

Tanaka, K.L., 1986. The stratigraphy of Mars. In: Proc. Lunar Planet. Sci. Conf. 17th, Part 1. J. Geophys. Res. 91 (suppl.) E139–E158.

Tanaka, K.L., Kargel, J.S., MacKinnon, D.J., Hare, T.M., Hoffman, N., 2002. Catastrophic erosion of Hellas basin rim on Mars induced by magmatic intrusion into volatile-rich rocks. Geophys. Res. Lett. 29 (8), doi:10.1029/2001GL013885.

Tanaka, K.L., Skinner, J.A., Hare, T.M., Joyal, T., Wenker, A., 2003. Resurfacing history of the northern plains of Mars based on geologic map-

ping of Mars Global Surveyor data. J. Geophys. Res. 108, doi:10.1029/2002JE001908.

Tanaka, K.L., Poruznick, T., Skinner, J.A., Hare, T.M., 2004. Geology of layered sequences in Arabia Terra, Mars. In: Second Conference on Early Mars. Abstract 8061.

Tanaka, K.L., Skinner, J.A., Hare, T.M., 2005. Geologic map of the northern plains of Mars. USGS Misc. Sci. Inv. Map 2888, scale 1:15,000,000.

Tokano, T., 2003. Spatial inhomogeneity of the martian subsurface water distribution: Implication from a global water cycle model. Icarus 164, 50–78.

Tsiganis, K., Gomes, R., Morbidelli, A., Levison, H.F., 2005. Origin of the orbital architecture of the giant planets of the Solar System. Nature 435, 459–461.

Turcotte, D.L., Schubert, G., 1982. Geodynamics: Applications of Continuum Physics to Geological Problems. Wiley, New York. 450 pp.

Turcotte, D.L., Willemann, R.J., Haxby, W.F., Norberry, J., 1981. Role of membrane stresses in the support of planetary topography. J. Geophys. Res. 86, 3951–3959.

US Geological Survey, 1991. Topographic map of Mars. USGS Misc. Inv. Ser. Map I-2179 (1:25,000,000).

Watters, T.R., 1988. Wrinkle ridge assemblages on the terrestrial planets. J. Geophys. Res. 93, 15599–15616.

Watters, T.R., Maxwell, T.A., 1986. Orientation, relative age, and extent of the Tharsis plateau ridge system. J. Geophys. Res. 91, 8113–8125.

Willemann, R.J., Turcotte, D.L., 1982. The role of lithospheric stress in the support of the Tharsis rise. J. Geophys. Res. 87, 9793–9801.

Wise, D.U., Golombek, M.P., McGill, G.E., 1979. Tharsis province of Mars: Geologic sequence, geometry, and a deformation mechanism. Icarus 38, 456–472.

Whitaker, E.A., 1981. The lunar Procellarum basin. In: Multi-Ring Basins. Proc. Lunar Sci. Conf. XIIA, 105–111.

Wohletz, K.H., Sheridan, M.F., 1983. Martian rampart crater ejecta: Experiments and analysis of melt-water interaction. Icarus 56, 15–37.

Wood, C.A., Head, J.W., Cintala, M.J., 1978. Interior morphology of fresh martian craters: The effects of target characteristics. Proc. Lunar Sci. Conf. IX, 3691–3709.

Yuan, D.N., Sjorgren, W.L., Konopliv, A.S., Kucinskas, A.B., 2001. Gravity field of Mars: A 75th degree and order model. J. Geophys. Res. 106, 23377–23401.

Zuber, M.T., Solomon, S.C., Phillips, R.J., Smith, D.E., Tyler, G.L., Aharonson, O., Balmino, G., Banerdt, W.B., Head, J.W., Johnson, C.L., Lemoine, F.G., McGovern, P.J., Neumann, G.A., Rowlands, D.D., Zhong, S., 2000. Internal structure and early thermal evolution of Mars from Mars Global Surveyor topography and gravity. Science 287, 1788–1793.